Terrestrial Sources and Sinks of Atmospheric Methyl Bromide: Three-Dimensional Modeling of Tropospheric Abundance and Sensitivities

Christopher D. Jensen

Department of Earth, Atmospheric and Planetary Sciences
MIT, Cambridge, MA 02139-4307 USA

Report No. 62
April 1999

The Earth's unique environment for life is determined by an interactive system comprising the atmosphere, ocean, land, and the living organisms themselves. Scientists studying the Earth have long known that this system is not static but changing. As scientific understanding of causal mechanisms for environmental change has improved in recent years there has been a concomitant growth in public awareness of the susceptibility of the present environment to significant regional and global change. Such change has occurred in the past, as exemplified by the ice ages, and is predicted to occur over the next century due to the continued rise in the atmospheric concentrations of carbon dioxide and other greenhouse gases.

The *Center for Global Change Science* at MIT was established to address long-standing scientific problems that impede our ability to accurately predict changes in the global environment. The Center is interdisciplinary and involves both research and education.

This report is one of a series of reports and preprints from the Center intended to communicate new results or provide useful reviews and commentaries on the subject of global change. See the inside back cover of this report for a complete list of the titles in this series.

Ronald G. Prinn, *Director*
Rafael L. Bras, *Associate Director*
Center for Global Change Science

For more information contact the Center office.

LOCATION:
Center for Global Change Science
Building 54, Room 1312
Massachusetts Institute of Technology
Cambridge, MA 02139-4307 USA

ACCESS:
Tel: (617) 253-4902
Fax: (617) 253-0354
E-mail: globalchange@mit.edu
World Wide Web: http://web.mit.edu/cgcs/www/

Printed on recycled paper

Terrestrial Sources and Sinks of Atmospheric Methyl Bromide: Three-Dimensional Modeling of TroposphericAbundance and Sensitivities

Christopher D. Jensen[†]

Abstract

Current estimates of methyl bromide surface fluxes are inconsistent with the observed tropospheric mole fractions (9 to 10 ppt, globally averaged) and the calculated atmospheric lifetime (1.7 ± 0.2 years), with mid-range estimates of sinks exceeding sources by at least 50 Gg y^{-1}. Given the uncertainties in process-specific surface flux estimates, we consider several distributions of terrestrial sources and sinks that satisfy the constraints on atmospheric abundance. Mole fractions corresponding to each distribution are simulated with a three-dimensional chemical transport model based on analyzed observed winds, coupled to a simple model of the ocean mixed layer. All of the resulting scenarios overestimate the observed zonal gradient, with interhemispheric ratios ranging from 1.39 to 1.60. In the absence of unknown sources, model results imply a biomass burning source near the upper limit of the range of present estimates (50 Gg y^{-1}). Sensitivities to surface fluxes are also calculated to determine the extent to which uncertain terms in the methyl bromide budget can be better quantified using long-term measurements. Results show that a global network capable of accurately monitoring the monthly, zonal mean distribution of CH_3Br would be able to distinguish between biomass burning fluxes and other known terrestrial sources and sinks. Modeled sensitivities to biomass burning emissions also highlight the importance of including tropical locations in any long-term monitoring network. However, technological sources and soil sinks have similar zonal patterns, and long-term, "background" mole fractions are relatively insensitive to zonal flux distributions. It is only when we examine the high frequency variability of the concentration that the effect of longitudinal gradients in the flux field becomes apparent.

Contents

[†] Submitted to the M.I.T. Department of Earth, Atmospheric, and Planetary Sciences on May 7, 1999 in partial fulfillment of the requirements for the degree of Master of Science in Atmospheric Science.

Terrestrial Sources and Sinks of Atmospheric Methyl Bromide: Three-Dimensional Modeling of Tropospheric Abundance and Sensitivities

by

Christopher D. Jensen

B.A., Environmental Chemistry, University of California, San Diego
(1996)

Submitted to the Department of Earth, Atmospheric and Planetary Sciences in partial fulfillment of the requirements for the degree of

MASTER OF SCIENCE
IN ATMOSPHERIC SCIENCE

at the

MASSACHUSETTS INSTITUTE OF TECHNOLOGY
May 1999

Signature of Author _____
Program for Atmospheres, Oceans, and Climate
May 1999

Certified by _____
Ronald G. Prinn
Professor of Atmospheric Chemistry
Thesis Supervisor

Accepted by _____
Ronald G. Prinn
Head, Department of Earth, Atmospheric, and Planetary Sciences

1. INTRODUCTION

Methyl bromide is the most abundant bromine-containing species in the free troposphere and the most important source of bromine atoms in the lower stratosphere [WMO, 1999; Kourtidis *et al.*, 1998; Lal *et al.*, 1994]. The resulting impact on stratospheric ozone has led to an international agreement to restrict future sales and consumption of methyl bromide for agricultural and industrial uses. However, unlike other ozone-depleting species subject to regulation under the Montreal Protocol, non-industrial surface fluxes play an important role in determining the atmospheric burden of methyl bromide. Despite efforts to understand the processes controlling the atmospheric budget of CH_3Br, the magnitude and distribution of fluxes remain poorly characterized.

At present, typical mid-range estimates of known sinks exceed sources by more than 80 Gg yr^{-1} [WMO, 1999]. This imbalance is inconsistent with the slow or negligible rate of change of observed tropospheric methyl bromide abundance [Khalil *et al.*, 1993; Miller, 1998; P. Simmonds and S. O'Doherty, University of Bristol, unpublished data]. However, surface flux estimates are based on the extrapolation of a relatively small number of measurements to a global scale, and an inevitably wide range of values results (with the sum of known fluxes ranging from –315 to 36 Gg yr^{-1} [WMO, 1999]). In addition, it is impossible to preclude the existence of a currently unidentified source that would balance the budget.

In situ measurements of CH_3Br mole fraction, in conjunction with an atmospheric chemical transport model (CTM) and optimal estimation techniques, could provide important constraints on the spatial and seasonal distribution of methyl bromide fluxes. However, the present catalog of atmospheric observations is small due to a combination of historical developments, funding constraints, and technical limitations [P. Simmonds, U. of Bristol, personal communication; S. Montzka, NOAA-CMDL, personal communication]. Despite these restrictions, the scientific and economic importance of understanding the biogeochemistry of methyl bromide motivate efforts to measure and model the atmospheric distribution of the gas.

Recent studies have focused on the global and hemispheric mass balance of methyl bromide [*e.g.*, Wingenter *et al.*, 1998; Lee-Tayor *et al.*, 1998]. In addition, the role of air-sea exchange in the atmospheric budget has been the subject of a number of modeling studies [*e.g.*, Butler, 1994; Yvon-Lewis and Butler, 1996; Anabar *et al.*, 1996; Pilinis *et al.*, 1996] and intensive field measurement campaigns [*e.g.*, Lobert *et al.*, 1995, 1996, 1997; Grozko and Moore, 1998]. However, few attempts have been made to justify assumptions about terrestrial sources and sinks of methyl bromide on a global scale.

Here, we evaluate the terrestrial budget of methyl bromide using a three-dimensional chemical transport model. The framework for doing so is straightforward. We observe that there is no conclusive evidence of an interannual trend in methyl bromide concentrations. Therefore, globally integrated sources must be equal or nearly equal to sinks. However, based on current understanding of the methyl bromide budget, sinks dramatically exceed sources. Thus, we must propose an additional, unknown source, or we must adjust known sources and sinks in a manner that will approximately reproduce ambient mole fractions. Several plausible combinations of sources and sinks are compiled, and the resulting methyl bromide distribution is estimated using a global CTM. Comparison of model results with observations yields insight into the relative

likelihood of each scenario. In addition, sensitivity to different sources and sinks is explored, which allows us to evaluate the ability of an improved network of long-term monitoring sites to reduce uncertainty in the methyl bromide budget.

2. ATMOSPHERIC MODEL

Long-term measurements of methyl bromide surface mole fraction indicate significant high frequency variability [P. Simmonds and S. O'Doherty, U. of Bristol, unpublished data] and meridional gradients [Miller, 1998]. Accurate simulation of steep spatial and temporal gradients requires a three-dimensional atmospheric model with realistic large-scale transport and adequate parameterizations of sub-grid scale processes. Existing global atmospheric transport models fall into two broad categories based on their treatment of large-scale advection: "climate models," which numerically solve the Navier-Stokes and thermodynamic equations to predict wind velocities, and "chemical transport models" (CTMs), which rely on archived meteorological center reanalysis data to predict large-scale transport. While both types of models have been widely used to simulate monthly and annual mean tropospheric abundance of trace species, comparisons with observations of chloroflurocarbons (CFCs) and radon indicate that only CTMs are capable of reproducing high frequency, *in situ* measurements [Hartley and Prinn, 1993; Mahowald, 1996; Mahowald *et al*., 1997a, 1997b]. The desire to understand both the long- and short-term variability of methyl bromide therefore motivates the choice of a CTM for this study.

We choose the Model for Atmospheric Transport and Chemistry (MATCH). The National Center for Atmospheric Research (NCAR), together with university collaborators, developed MATCH for the purpose of modeling trace gas distributions in the troposphere. Mahowald *et al.* [1997a, 1997b] validate the accuracy of MATCH for species with atmospheric lifetimes substantial longer and shorter than CH_3Br ($CFCl_3$ and ^{222}Rn, respectively). The tracers in these studies have relatively well constrained sources and sinks, and therefore provide a revealing test of the model's transport scheme. MATCH simulated monthly mean transport with some success globally, and was able to diagnose some aspects of synoptic-scale variability at mid-latitudes. Correlation coefficients between daily average, *in situ* measurements and model output ranged from 0.25 to 0.86. In general, agreement was best at mid-latitude stations and (especially for the $CFCl_3$ simulation) poor in the tropics. Although some discrepancies are apparent in monthly mean $CFCl_3$ (CFC-11) values, most simulated mole fractions fell within the standard error of the measurements (see Mahowald *et al.,* 1997a).

A detailed description of MATCH is available in the previously cited papers. This study makes use of an updated version of the model described in Lawrence *et al.* [1998a, 1998b]. Advection is based on the mass-conserving SPITFIRE (Split Implementation of Transport using Flux Integral Representation) algorithm developed by Phil Rasch of NCAR [Rasch and Lawrence, 1998]. Vertical diffusion is derived from the non-local boundary layer scheme of Holtslag and Boville [1993]. Moist convection is calculated using the Zhang/McFarlane/Hack parameterization derived from the CCM3 climate model [Zhang and McFarlane, 1995; Hack, 1994]. This approach successively applies the Zhang/McFarlane bulk plume model, followed by the Hack scheme, which removes any remaining convective instability. Temperature, pressure, humidity, and wind data are derived from NCEP reanalysis archived at T62 (192 x 94 grid

points) resolution, with optional integration to a T42 (128 x 64) grid. Variables are input at six-hour intervals and at 28 σ-levels ranging from 0.0027 to 0.995, with 18 levels below 200 hPa.

The atmospheric chemistry of methyl bromide is dominated by reaction with the hydroxyl radical in the troposphere and photolysis the stratosphere. We define the OH distribution using monthly-average outputs from the three-dimensional MATCH-MPIC model of Lawrence *et al.*, [1998a, 1998b] (see also Lawrence, 1996). MATCH-MPIC version 1.2 and version 2.0 results are averaged for the purpose of this study. Because lower tropospheric OH values tend to be higher over continental regions, the OH field is weighted toward the Northern Hemisphere, with a mean tropospheric interhemispheric OH ratio of 1.27. This is consistent with some recent two-dimensional model results of [*e.g.*, Wang *et al.*, 1998]. However, the OH distribution of Prinn *et al.* [1995], widely used as a basis for lifetime estimates of long-lived gases, is approximately symmetric about the equator [J. Huang, MIT, personal communication]. The deviation from the Prinn *et al.* [1995] distribution may bias the model toward unrealistically low interhemispheric ratios.

Reaction rates with OH are taken from DeMore *et al.* [1997]. Loss due to $O(^1D)$ and tropospheric photolysis are ignored. Stratospheric destruction frequencies (*J*-values) for CH_3Br have been calculated using the spectral model described in Golombek and Prinn [1986, 1993]. Results from the spectral model indicate a lifetime against stratospheric photolysis of 33 years [A. Golombek, MIT, personal communication], in close agreement with the estimate of WMO [1999] (35 years). Implementation of tropospheric oxidation and stratospheric photolysis in MATCH is discussed in greater detail in Section 4.

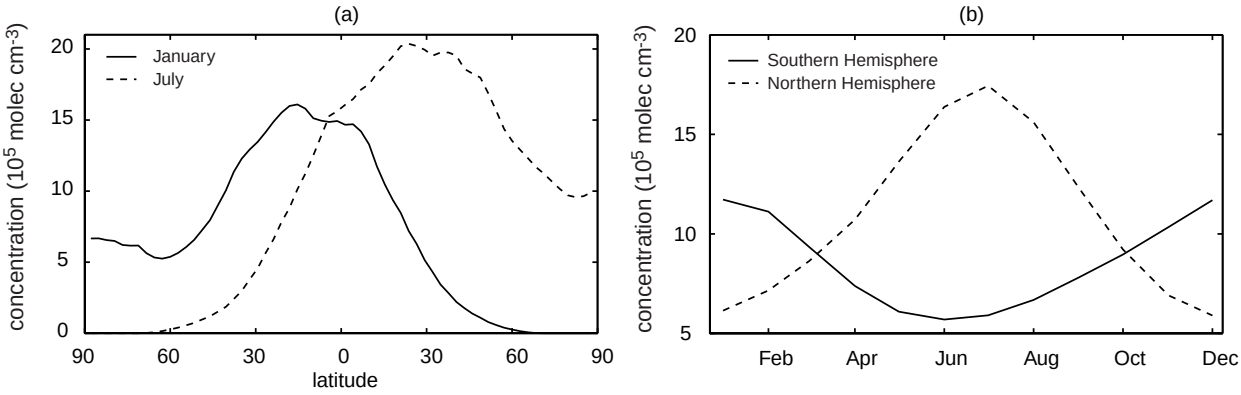

Figure 2.1. OH concentrations from Lawrence *et al*. [1997a]. (a) Zonal mean tropospheric mole fractions. Solid line, January value; dashed line, July value. (b) Monthly mean tropospheric mole fractions. Solid line, Southern Hemisphere; dashed line, Northern Hemisphere.

3. SOURCES AND SINKS: Estimates from Process-based Studies

Reported sources and sinks of methyl bromide include technological uses, marine production and consumption, deposition to soils, biomass burning, combustion of leaded fuel, oxidation by the hydroxyl radical, and stratospheric photolysis. An estimate of the magnitude of each process is compiled from published field studies, laboratory measurements, and modeling exercises. Spatial, and when possible, seasonal distributions are assigned for each process. A mid-range

value is obtained from literature references and modeling of the physical processes involved. In general, rigorous estimates of the uncertainties are not available. However, an attempt is made to inform the reader of reported ranges and standard errors in the cited literature, while noting the criteria for such estimates vary widely among authors.

3.1 Fumigation and Industrial Sources

The largest sources of methyl bromide are currently believed to be from agricultural and industrial applications. Methyl bromide is a broad-spectrum pesticide that is primarily used as a soil fumigant in the cultivation of high value-added agricultural products (*e.g.*, truck crops), as a structural fumigant, and as a fungicide during the transport and quarantine of foodstuffs [WMO, 1999]. In 1996, industrialized nations accounted for approximately 80% of global sales and consumption [http://www.epa.gov/ spdpublc/mbr/ambtoc.html]. In addition, a smaller quantity of CH_3Br is used as a chemical intermediate in industrial processes.

The release of methyl bromide following soil fumigation is not well understood. The amount of gas reaching the atmosphere depends primarily on the depth of application, on whether a tarp was used to retard soil-to-air gas transfer, and on the soil temperature [Klein, 1996]. Estimates of release, typically expressed as the fraction of applied methyl bromide reaching the atmosphere, vary widely. Yagi *et al.* [1995] estimate that 34–87% of applied methyl bromide enters the atmosphere, while Reible [1994] estimate 26–65% of the applied mass escapes from the soil. Almost all emissions occur within two weeks of application [*ibid.*]. Seasonal variations in source strength are not well constrained. Lee-Taylor *et al*. [1998] cite observations by Miller and Weiss [1995] off the coast of California to argue for a bimodal distribution of local emissions corresponding to the planting of crops in the spring and fall. However, the implications of the Miller and Weiss measurements are uncertain [R.F. Weiss, personal communication; Miller, 1998], and local conditions that determine the timing of planting and harvest will effect methyl bromide emissions. Assuming a simple seasonal cycle is also likely to be unrealistic because the majority of methyl bromide is applied in Mediterranean and subtropical climates, which, like

Table 3.1. Methyl Bromide Consumption by End Use (1996)

End Use	Consumption (metric tons)	Percent of Category	Percent of Total
Developed	**56,108**		**82%**
Preplant	39,275	70%	
Durable	6,172	11%	
Perishable	4,820	9%	
Structural	3,254	6%	
Chemical Intermediate	2,531	5%	
Developing	**12,316**		**18%**
Preplant	8,621	70%	
Durable	2,463	20%	
Perishable	493	4%	
Structural	739	6%	
TOTAL	**68,424**		**100%**

Source: http://www.epa.gov/spdpublc/mbr/ambtoc.html

California, frequently produce more than one crop per year. In light of the uncertainties, we assume seasonally uniform methyl bromide emissions from soil fumigation, while realizing that there is likely to be significant seasonal variation in the actual budget. Commodity and structural fumigation applications result in more direct mixing between the atmosphere and the fumigant. Release to the atmosphere from these applications is expected to approach 100% of the applied mass. Emissions from non-fumigation industrial process (*e.g.*, fugitive emissions in chemical manufacturing) are small (less than 2 Gg yr^{-1} [WMO, 1995]) and are assumed to be seasonally invariant.

Sales and use of methyl bromide are relatively well quantified at the national level. Consumption estimates for the 1991 calendar year are available for 72 countries, which together account for approximately 96% of global CH_3Br sales [http://www.epa.gov/spdpublc/mbr/ambtoc.html]. Additional estimates for China, the Former Soviet Union, and India are taken from WMO [1995]. Estimates for use in soil fumigation are provided for 10 countries and six U.S. states, whose consumption totals 80% of global fumigation use. Soil fumigation is estimated at 70% of total consumption in remaining countries, and 50% of the applied fumigant is assumed to enter the atmosphere. Remaining sources are aggregated among four regions: the United States, other industrialized nations, the Former Soviet Union, and developing countries. Intra-regional distribution is assigned based on national energy consumption data [http://www.eia.doe.gov/emeu/international/] and is weighted within countries by the gridded population data of Li [1996]. This parameterization is chosen to reflect the level of economic activity within a particular grid cell. The resulting mid-range estimate of source strength is 44 Gg yr^{-1}. If only 25% of applied soil fumigant escapes to the atmosphere, the source is reduced to 33 Gg yr^{-1}. An 85% emissions factor increases estimated flux to 60 Gg yr^{-1}. Recent methyl bromide sales figures (see **Table 3.2**) place an upper limit on annual methyl bromide release of less than 70 Gg yr^{-1}. The mid-range estimate falls well within the range of 25 to 64 Gg yr^{-1} cited by Butler and Rogriguez [1996].

Table 3.2. Historical Sales of Methyl Bromide by Region (metric tons)

Year	North America	Europe	Asia	Other	Total Sales
1984	19,659	11,364	10,678	3,871	45,572
1985	20,062	14,414	9,743	4,054	48,273
1986	20,410	13,870	11,278	4,897	50,455
1987	23,004	15,339	12,816	4,531	55,690
1988	24,848	17,478	13,555	4,729	60,610
1989	26,083	16,952	14,386	5,149	62,570
1990	28,101	19,119	14,605	4,074	66,644
1991	31,924	18,020	17,396	6,260	73,600
1992	29,466	18,521	16,944	6,654	71,585
1993	30,723	18,286	17,185	6,463	72,658
1994	31,981	18,052	17,427	6,271	73,731
1995	28,965	16,350	15,784	5,680	66,778
1996	29,679	16,753	16,173	5,820	68,424

Source: http://www.epa.gov/spdpublc/mbr/ambtoc.html

3.2 Leaded Fuel Consumption

Leaded gasoline contains the additive 1,2-dibromoethane (EDB). In the combustion process, some of the bromine in EDB is converted to other organobromine species, including methyl bromide [Baumann and Heumann, 1987]. While sales of leaded fuel are relatively well constrained, a wide range of CH_3Br-to-Pb emissions ratios have been reported in motor vehicle exhaust. Published CH_3Br-to-Pb ratios [*ibid.*] imply motor vehicles are an important source of methyl bromide, contributing up to 22 Gg yr^{-1} to the atmospheric budget. However, more recent studies imply source strengths an order of magnitude lower [Baker *et al.*, 1998; Chen *et al.*, 1999].

Motor vehicle emissions of methyl bromide are calculated using lead emissions from the Global Emissions Inventory Activity (GEIA) database [http://www.info.ortech.on.ca/ cgeic/]. Applying the CH_3Br-to-Pb ratios of Baumann and Heumann [1987] results in an estimated source strength of 15.3 ± 5.6 Gg yr^{-1}, with uncertainties accounting for the stated range of emissions factors and lead emissions. However, more recent studies indicate that this estimate overstates emissions from motor vehicles by a factor of 1.3–10 [Baker *et al.*, 1998; Chen *et al.*, 1999; WMO, 1999]. In this study, the average of the high and low estimates (8.5 Gg yr^{-1}) defines the mid-range global emissions. However, any estimate from less than 1 to 15 Gg yr^{-1} could be justified using reported emissions factors [WMO, 1999].

3.3 Oceans

Air-sea exchange has long been recognized as an important element in the natural biogeochemical cycling of methyl bromide. To the present day, the influence of marine process on the atmospheric methyl bromide budgets remains uncertain. The confusion stems from the bi-directional nature of the air-sea exchange process and the sparseness of *in situ* flux measurements.

Biological processes in the ocean are known to produce a wide range of halogenated hydrocarbons, including methyl bromide [Manley and Dastoor, 1987; Scarratt and Moore, 1996]. Early field campaigns by Lovelock [1975] and Singh *et al.* [1983] found large supersaturations in pelagic regions. However, more recent modeling studies and ship-based measurements emphasize the importance of the oceanic sink due to hydrolysis in seawater

$$CH_3Br + OH^- \rightarrow CH_3OH + Br^-. \qquad \text{[Elliot and Rowland, 1993]}$$

Additionally, the substitution reaction with chloride ion to yield methyl chloride is an important sink

$$CH_3Br + Cl^- \rightarrow CH_3Cl + Br^-. \qquad \text{[}ibid.\text{]}$$

The total rate is strongly temperature dependent and can vary by more than an order of magnitude under environmental conditions [Anabar *et al.*, 1996]. Biological degradation is also thought to play an important role in the removal of methyl bromide from seawater [King and Saltzman, 1997].

Measurements in the Southern Ocean [Lobert *et al.*, 1997], the Eastern Pacific [Lobert *et al.*, 1995], and the Atlantic [Lobert *et al.*, 1996] have shown large regions of methyl bromide undersaturation. Supersaturation was observed only in coastal areas or in upwelling regions of the East Pacific [*ibid.*]. Extrapolating to a global scale, the authors calculate a net source of 3.5 Gg yr^{-1} in these areas of high biological productivity. However, the positive flux from coastal and upwelling regions is more than balanced by loss from the atmosphere to the open ocean [Lobert *et al.*, 1995].

The results of Lobert *et al.* [1995] are contradicted by several modeling studies [Anabar *et al.*, 1996; Pilinis *et al.*, 1996] that estimate a positive net global flux from the oceans to the atmosphere. However, subsequent *in situ* measurements by Grozko and Moore [1998, hereafter GM98], Lobert *et al.* [1997], and Moore and Webb [1996] cast doubt on a number of parameterizations used in the theoretical studies. More specifically, it became clear that the linear correlation between chlorophyll concentrations and biological methyl bromide production assumed in these models is not realistic.

Recent measurements by GM98 lend further support to the hypothesis that the oceans act as net sink for atmospheric CH_3Br. However, data collected in the North Atlantic and Central Pacific support the existence of a regional net source from pelagic waters within a narrow band of sea surface temperatures (SSTs) largely confined to temperate latitudes. GM98 suggests that saturation anomalies linearly increase with SST for temperatures less than 17 ˚C. For higher SSTs, a quadratic curve is fit to the data. Their relation can be represented by the equations:

$$A_{sat} = -1.5 + 0.124T \qquad T \le 17$$
$$A_{sat} = 7.846 - 0.642T + 0.0123T^2 \qquad T > 17$$

where T is the temperature in degrees Celsius and A_{sat} is the saturation anomaly in pmol L^{-1}. In this study, we apply the GM98 relation to climatological SSTs [Levitus *et al.*, 1994] to obtain an estimate of the spatial and seasonal variations in air-sea flux. The net flux to the atmosphere, F, is governed by the relation

$$F = \rho_a K_w (HC_o - \chi_a)$$

where ρ_a is the atmospheric density, χ_a is the atmospheric concentration in atm, C_o (mol m^{-3}) is the concentration of methyl bromide in the ocean mixed layer, H (atm m^3 mol^{-1}) is the Henry's law coefficient of CH_3Br in seawater, and K_w (m s^{-1}) is the air-sea exchange coefficient [Wanninkhof, 1992]. The time tendency of the marine CH_3Br abundance is given by

$$\frac{dC_o}{dt} = \frac{P_o}{z_o} - k_o C_o - \frac{K_w}{z_o}\left(C_o - \frac{\chi_a}{H}\right)$$

where z_o is the mixed layer depth, P_o is the net biological production of methyl bromide in the mixed layer, and k_o is the combined loss rate due to eddy degradation, biological uptake, and chemical loss [Butler, 1994].

King and Saltzman [1997] and Butler [1994] define the first-order rate constant k_o. The mixed layer depth is archived by the Integrated Global Ocean Services System (IGOSS) [http://ingid.ldeo.columbia.edu/]. K_w and H are functions of sea surface temperature and salinity and can be computed from hydrographic data using empirical expressions determined by DeBruyn and Saltzman [1997a, 1997b]. K_w is also strongly dependent on wind speed (U). Wanninkhof [1992] reviews parameterizations of air-sea exchange and suggests the relation

$$K_w = kU^2\left(\frac{S_c}{660}\right)^{-0.5}$$

where S_c is the Schmidt number, which is a function of temperature and chemical species, and k is a proportionality constant. Liss and Merlivat [1986] propose an alternative, piecewise linear form for the dependence of the air-sea transport rate on wind speed.

Using monthly climatological values for the mixed layer depth, solubility, sea surface temperature, and wind speed [DaSilva *et al.*, 1994], along with the saturation anomaly parameterization of GM98, the steady state estimate of net biological production is given by

$$P_o = k_o\, z_o\, C_o + K_w\, A_{sat}$$

$$A_{sat} = \left(C_o - \frac{\chi_a}{H} \right)$$

i.e., biological production is balanced by *in situ* loss and net flux to the atmosphere. Assuming mole fractions of 8.6 and 11.0 ppt in the Northern and Southern Hemispheres, respectively [S. Montzka, unpublished data], the parameterization yields an *a priori* estimate of the global net flux of –5.6 Gg yr^{-1} (positive indicating a flux to the atmosphere). The net sink is almost equally distributed between the Northern and Southern hemispheres. Note that this choice of parameterization also qualitatively agrees with observations of regional features such as the large negative saturation anomalies found in the Southern Ocean [Lobert *et al.*, 1997], and the seasonal supersaturation in the North Atlantic reported in Baker *et al.* [1999]. However, the magnitude of the global net sink is one-fourth the value reported by Lobert *et al.* [1997], and 40% less than that calculated by GM98 using zonally and annually averaged hydrographic data.

The global flux is also sensitive to the parameterization of the piston velocity. The Liss and Merlivat [1986] scheme yields a global net flux of –2.8 Gg yr^{-1}, one-half the value obtained with the Wanninkhof [1992] parameterization. Additionally, one must assume that the biological productivity and saturation anomalies have ecosystem-dependent terms that are not reflected in the treatment of GM98. However, the pattern of fluxes is qualitatively consistent with observed air-sea exchange.

3.4 Biomass Burning

Vascular plants contain between 1–100 ppm by weight bromine [McKenzie *et al.*, 1996]. During wildfires, the burning of agricultural fields, or the burning of biomass for fuel, some percentage of the bromine reacts to form methyl bromide. Globally, this is estimated to release 10 to 50 Gg yr^{-1} of CH_3Br to the atmosphere [Manö and Andreae, 1994]. The amount of methyl bromide emitted depends on the composition of the standing biomass and the intensity of the fire. Measured CH_3Br-to-CO_2 emissions ratios range from 0.46 x 10^{-6} for savanna fires to 1.30 x 10^{-6} for boreal forest fires [*ibid.*].

Globally, fire emissions are divided into two categories: hot/low emissions fires (savanna fires, agricultural residue burning) and cool/high emissions fires (forest fires, fuel wood burning), with the appropriate emissions ratios assigned to each category. Tropical biomass burned is calculated from the database of Hao and Liu [1994], who estimate dry matter burned from four fire types: forest fires, savanna fires, agricultural field clearance, and domestic fuel wood consumption, with forest and savanna fire emissions provided at monthly resolution. No direct estimate of temperate or boreal forest fire biomass burned is available, but standing biomass estimates of Olson *et al.* [1985] and fire frequencies estimated by Seiler and Crutzen [1980] can be combined to determine an annual carbon flux from non-tropical forest fires. A late summer burning season is assumed in temperate latitudes, lasting three months (Jul-Sep) in the Northern Hemisphere and four months in Australia (Dec-Mar). Other extratropical fires are

unlikely to be significant components of the methyl bromide budget and are ignored. The percentage of carbon released as CO_2 is calculated from CO-to-CO_2, CH_4-to-CO_2, and NMHC-to-CO_2 ratios of Granier *et al.* [1996]. Combined with the CH_3Br-to-CO_2 ratios described above, a magnitude and pattern can be estimated for methyl bromide emissions. Total global emissions are estimated 14.6 Gg yr^{-1}, with all but 0.8 Gg yr^{-1} originating in the tropics. Peak burning periods occur in the dry tropics in the boreal spring (Northern Hemisphere) and boreal fall (Southern Hemisphere).

The global estimate is near the low end of the 10 to 50 Gg yr^{-1} range of Manö and Andreae [1994]. This is due primarily to the lower-than-average biomass burning estimate of Hao and Liu [1994]. While Hao and Liu [1994] estimate that 5390 Tg yr^{-1} of dry biomass is burned annually in the tropics, Crutzen and Andreae [1990] estimate a range of 4000–10,450 Tg yr^{-1}. A 40% increase in the Hao and Liu [1994] biomass burning flux would yield methyl bromide emissions consistent with the consensus mid-range value of 25 Gg yr^{-1} [WMO, 1999]. Additional uncertainty due to the estimate of CH_3Br-to-CO_2 emissions ratios (estimated to be a factor of three by Manö and Andreae [1994]) and interannual variability of biomass burning must be considered, as well. Nonetheless, the basic spatial and seasonal pattern of biomass burning emissions, dominated by burning in the seasonally dry tropics, seems likely to remain intact despite large (greater than 100%) uncertainties in the magnitude of the flux. For model runs discussed in Section 4, a mid-range flux estimate of 25 Gg y^{-1} is used based on the probable underestimate of the biomass burning rate by Hao and Liu [1994]. Distribution is determined based on the parameterization discussed above.

3.5 Soil Sinks

Oremland *et al.* [1994] demonstrate under laboratory conditions that soil-dwelling methanotrophic bacteria consume significant amounts of methyl bromide at superambient CH_3Br mole fractions (greater than 10 ppm). Subsequent studies of natural and agricultural soils indicate that soils are an important sink for methyl bromide at ambient partial pressures [Shorter *et al.*, 1995; Serca *et al.*, 1998]. Published estimates of global loss rates range from 42 ± 32 Gg yr^{-1} [Shorter *et al.*, 1995] to 140 Gg yr^{-1} [Serca *et al.*, 1998]. A large part of the difference between the studies is due to different geographical classifications of soil and vegetation type employed by the two authors [*ibid.*]. With the exception of agricultural soils, which constitute almost half of the flux calculated by authors of the later study but only 6% of that from the Shorter *et al.* [1995] paper, estimated deposition rates agree within 20%.

We combine the measured fluxes from Shorter *et al.* [1995] with the land use data of Matthews [1983] to produce an *a priori* estimate of global soil fluxes. The lower estimate of Shorter *et al.* [1995] is chosen for several reasons. First, the actual difference in deposition velocities measured by Shorter *et al.* [1995] and Serca *et al.* [1998] are relatively small, with the exception for deposition to agricultural soils. Second, the Serca *et al.* [1998] estimate for global loss to soils, if correct, would imply an even more dramatic imbalance in the methyl bromide budget. The resulting gridded data yields a mid-range estimate of the global soil flux of –33 Gg yr^{-1}, 20% less than the mid-range estimate of Shorter *et al.* [1995]. A seasonal cycle is determined by assuming growing seasons of 180, 240, and 360 days in boreal, temperate, and tropical regions, respectively.

3.6 Photochemical Loss

The main sink of methyl bromide in the troposphere is oxidation by the hydroxyl radical

$CH_3Br + OH \rightarrow CH_2Br + H_2O$.

A small fraction of the atmospheric burden is also lost to photolysis in the stratosphere. The partial lifetimes against oxidation and photolysis are estimated at 1.8 ± 2 years and 35 years, respectively [Butler and Rodriguez, 1996; WMO, 1999]. This implies a global loss rate of 86 Gg yr^{-1} (with a range from 72 to 101 Gg yr^{-1}) for mean global mole fractions of 9 to 10 ppt [WMO, 1999].

3.7 Terrestrial Vegetation

The persistent imbalance of methyl bromide sources and sinks has led to several recent studies examining the role of higher plants in the global budget. Gan *et al.* [1998] find relatively large emissions from wild and cultivated members of the genus *Brassica*, and estimate global emissions from rapeseed of 6.6 ± 1.6 Gg y^{-1}. Another study, by Jeffers and Wolfe [1998], presents evidence that the leaves, roots, and stems of plants may be a small, but measurable, sink of atmospheric CH_3Br. In the absence of a net marine source or a large underestimate of known terrestrial sources, it is tempting to assume a significant CH_3Br source from natural or agricultural vegetation in order to balance the global budget. However, evidence for a net positive flux is mixed. A hypothetical source from natural vegetation is simulated in Section 4 for the purpose of informing the continued discussion of the subject.

Table 3.3. Reference Methyl Bromide Fluxes

Source/Sink	Net Flux (Gg y^{-1})	Range (Gg y^{-1})
Agricultural/Industrial	44	33 to 60
Lead fuel combustion	8.5	0 to 15
Biomass burning	25	10 to 50
Soil deposition	–33	–140 to –10
Air-sea exchange	–5.6	–30 to –3
Photochemical loss	–86	–101 to –72
Total	**–47**	**–228 to 40**

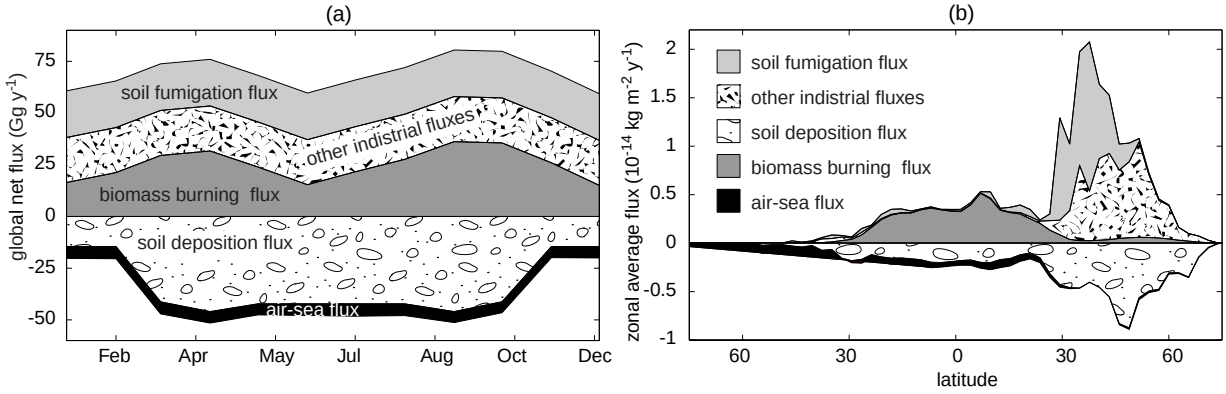

Figure 3.1. Reference net surface flux values for soil fumigation, other industrial, biomass burning, soil deposition and air-sea exchange. (a) Monthly mean global flux. (b) Annually averaged zonal mean flux. Areas of polygons above zero flux value represent net sources. Areas of polygons of below zero flux value represent net sinks. Upper and lower envelopes represent the sum of the net surface sources (positive values) and the net surface sinks (negative values).

4. ATMOSPHERIC ABUNDANCE: Modeling Ambient Tropospheric Mole Fractions

Process-based flux estimates are an important starting point for the characterization of the atmospheric methyl bromide budget. However, several limitations are immediately apparent. First, the uncertainty of the flux estimates is large, often more than a factor of two for a specific process. Second, the mid-range process-based flux estimates are not balanced, with sinks outweighing sources by a wide margin. Although long-term measurements of methyl bromide are sparse, there is widespread agreement that any interannual trend in mole fractions is insignificant or only slightly upward over the last 15 years [Cicerone *et al.*, 1988; Miller *et al.*, 1998; Khalil *et al.*, 1993; P. Simmonds and S. O'Doherty, U. of Bristol, unpublished data]. It is therefore quite reasonable to attempt to formulate a balanced budget that attempts to reproduce observed tropospheric mole fractions of 9–10 ppt [WMO, 1999]. This can be done by increasing the magnitude of existing sources, decreasing that of known sinks, and/or introducing a currently unrecognized source.

Given the wide uncertainties in physical parameters, there is clearly more than one choice of parameters which would produce a balanced budget. Several such choices are considered here. MATCH is then used to simulate atmospheric methyl bromide mole fractions, and the results are compared with available measurements. Estimation of the parameters controlling source and sink distribution is best approached as an inverse problem, in which an optimization is performed to determine the values that most closely fit the data. The publication of several important databases of long-term measurements should soon increase the attractiveness of optimal estimation techniques to researchers studying atmospheric methyl bromide [P. Simmonds, U. of Bristol, personal communication; S. Montzka, NOAA-CMDL, personal communication; see also Miller, 1998]. At the moment, however, the problem almost certainly is too severely underdetermined to produce meaningful results. Nonetheless, the path from the sensitivity studies described herein to a formal inverse estimate of surface flux values is simple and direct.

Before describing these sensitivity studies further, it is best to pause and consider which parameters the model is not sensitive to, as well as the parameters we choose to hold constant in order to simplify our conceptual framework. First, the partial lifetimes due to oxidation by OH and stratospheric photolysis are taken to be 1.8 years and 35 years respectively [WMO, 1999]. Two three-dimensional CTM runs, which produce significantly different vertical distributions of the hydroxyl radical, are averaged to determine the initial OH field (see Lawrence *et al.*, 1998a). The initial values are multiplied by a factor 1.06 in order to reproduce the consensus lifetime estimate. MATCH does not accurately simulate stratospheric dynamics and chemistry. A three-dimensional spectral model with a well-resolved stratosphere [Golombek and Prinn, 1986, 1993; A. Golombek, MIT, personal communication] closely reproduces the WMO [1999] estimated lifetime against stratospheric photolysis (35 years). However, uncalibrated MATCH runs using *J*–coefficients extrapolated from the spectral model result in a lifetime against photolysis of approximately 10 years, and a large correction factor is required to reproduce the WMO [1999] value. The effect of this correction on tropospheric mole fractions is small.

In addition, the parameterization of GM98 implies a relatively small, negative net flux to the ocean. This assumption is maintained in all simulations. The role of oceans in the biogeochemical cycling of methyl bromide has been discussed at length elsewhere [*e.g.*, GM98; Lobert *et al.*, 1995,

1996, 1997; Anabar *et al.*, 1996; Pilinis *et al.*, 1996; Bulter, 1994; Yvon-Lewis and Butler, 1996]. Using the air-sea flux estimate of Lobert *et al.* [1995, 1996, 1997] would require a larger net terrestrial source to balance the budget. This option is not considered here. Instead, we couple the ocean mixed layer model discussed in Section 3.3 to MATCH. Marine biological production is defined by its steady state, climatological value, and air-sea exchange is governed by the parameterization for instantaneous wind speeds of Wanninkhof [1992]. This formulation preserves the essential characteristics of the GM98 saturation anomaly parameterization, while allowing the air-sea flux to evolve more realistically in response to changing atmospheric concentrations.

Of the terrestrial processes thought to be important in the global budget, the role of leaded fuel combustion is not considered in a systematic fashion. The strength of the emissions is held constant in all scenarios, at 8.5 Gg yr^{-1}, the average of the Baker *et al.* [1998] and Baumann and Heumann [1987] estimates. While this masks large uncertainty in the chemistry of the combustion process (the cited estimates differ by a factor of 10), in fact atmospheric methyl bromide concentrations are unlikely to be strongly sensitive to the CH_3Br-to-Pb emissions ratio on larger-than-local scales.

In summary, we hold leaded fuel emissions, marine physical and biological parameters, and atmospheric lifetimes constant. The independent variables in our system are therefore technological emissions, biomass burning emissions, and deposition to natural and agricultural soils. The first category can be further divided between structural, commodity, and industrial emissions, which are relatively well constrained (certainly within less than a factor of two), and emissions from soil fumigation applications, which are highly uncertain. **Table 4.1** outlines the input parameters used to produced a roughly "balanced" methyl bromide budget. In addition, we propose a hypothetical unknown source with a magnitude of 50 Gg yr^{-1} and a distribution proportional to monthly average Pathfinder AVHRR normalized difference vegetation index (NDVI) [http:// daac.gsfc.nasa.gov/CAMPAIGN_DOCS/LAND_BIO/GLBDST_Data.html]. This is considered as a thought exercise, but it is likely to reproduce some of the broader characteristics of any (admittedly unknown) ubiquitous release of methyl bromide from terrestrial higher plants.

Table 4.1. Model Run Parameters

Model Runs		Biomass burning flux (Gg y^{-1})	Soil fumigation flux (Gg y^{-1})	Deposition velocity (% reference*)	Other
Reference run:	MMM	25	22.5	100	
Balanced runs:	HLM	50	22.5	30	NA
	HMH	50	42.8	100	NA
	MLH	25	42.8	30	NA
	VEG	25	22.5	100	50 Gg y^{-1} from vegetation
Fumigation	NA	50	22.5	30	industrial source, N. America[1]
Sensitivity runs:	EUR	50	22.5	30	industrial source, Eusasia[2]
	LEE	50	22.5	30	seasonal fumigation cycle
High Biomass	XMM	70	22.5	100	NA
Burning runs:	XML	80	11.3	100	NA
	XHM	90	22.5	170	NA

* Reference deposition velocity defined by Shorter *et al.* [1995].
[1] Industrial source 10 Gg y^{-1} higher in North America.
[2] Industrial source 10 Gg y^{-1} higher in Eurasia.

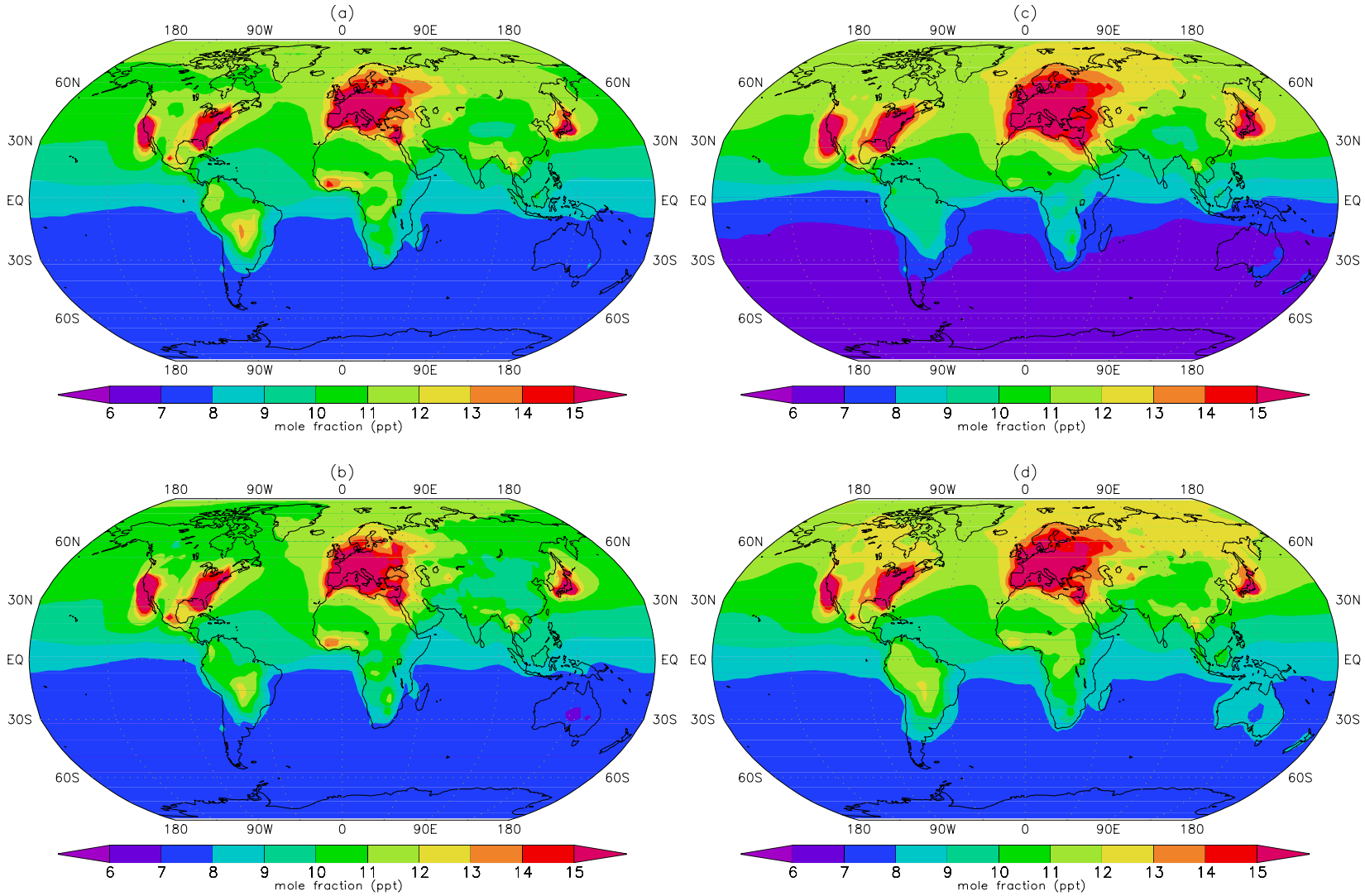

Figure 4.1. Annual average methyl bromide surface mole fraction from balanced MATCH runs. (a) Model run HLM, (b) HMH, (c) MLH, (d) VEG.

In addition, a reference case based on mid-range emissions estimates is included. This is not "balanced," in the sense that steady state mole fractions are substantially lower than observed atmospheric values.

Upon completion of the "balanced budget" runs, several major deficiencies in the simulation of surface mole fraction became apparent. These issues will be discussed at length in Section 5. Briefly, the balanced runs overestimate observed interhemispheric ratios by 10% or more, and underestimate the observed (positive) gradient between Trinidad Head, California and Mace Head, Ireland by 7 to 10%. In an attempt to better understand these discrepancies, two new sets of emissions scenarios are considered, and their corresponding mole fraction distributions are simulated by MATCH. First, we address the issue of the California-to-Ireland gradient by recognizing that the primary determinant of zonal variability in the northern mid-latitudes is the large, longitudinally heterogeneous technological source. Mole fractions in Ireland and California are estimated using several different spatial and temporal distributions of technological emissions. Using the mid-range estimate for total agricultural and industrial sources, emissions are redistributed to assign an additional 10 Gg y^{-1} flux to North America (run NA) or Eurasia (run EUR). We also test a bimodal seasonal distribution of soil fumigation emissions after Lee-Taylor *et al.* [1998] (run LEE).

A second set of runs is constructed in an attempt to better simulate observed zonal gradients. Of the known sources, only the biomass burning flux is significant in the Southern Hemisphere, where emissions represent approximately 40% of the global total. Therefore, to reduce the zonal gradient within the theoretical framework of the model, we must increase biomass burning fluxes above the 50 Gg y^{-1} maximum value cited by Manö and Andreae [1994]. Several runs with biomass burning sources in excess of 50 Gg y^{-1}, balanced by lower agricultural sources and/or higher soil sinks, are discussed in Section 5. Input parameters for the "high biomass burning" runs are included in Table 4.1.

5. MODEL RESULTS AND COMPARISON WITH OBSERVATIONS

The MATCH model is run to within one percent of interannual steady state using 1995 NCEP reanalysis data integrated to T42 resolution. Results are summarized in **Tables 5.1** and **5.2**. Note the partial lifetime against air-sea exchange is long relative to accepted values, for reasons discussed above. Also, lifetimes against soil deposition are at the upper end of the range of Shorter *et al.* [1995], and are considerably longer than those of Serca *et al.* [1998].

For "balanced budget" runs, global surface mean mole fraction falls within the accepted range of 9–10 ppt [WMO, 1999]. The annually averaged interhemispheric ratio exceeds reported values by 10 to 40% [Lobert *et al.*, 1995; Grozko and Moore, 1998; Wingenter *et al.*, 1998;

Table 5.1. Results from Balanced Model Runs

	HLM	HMH	MLH	VEG
Atmospheric burden (Gg)	134	132	130	138
Mean surface mole fraction (ppt)	9.3	9.2	9.2	9.7
NH surface mole fraction (ppt)	10.9	10.9	11.3	11.3
SH surface mole fraction (ppt)	7.8	7.6	7.1	8.0
Surface interhemispheric ratio	1.39	1.44	1.60	1.41

Table 5.2. Lifetimes (years) from Balanced Model Runs

	HLM	HMH	MLH	VEG
$\tau_{atmosphere}$	1.7	1.7	1.7	1.7
τ_{ocean}	22.8	19.6	22.8	19.2
τ_{soil}	26.1	6.0	20.1	5.8
τ_{total}	1.5	1.2	1.5	1.2

Miller, 1998]. Disagreement is largest in the boreal winter, and is most pronounced in run MLH. The treatment of soil and ocean sinks leads to an atmospheric lifetime estimate 70 to 110% higher than the mid-range value reported by WMO [1999] (0.7 years).

5.1 Time Series Observations and Model Results

Several long-term records of surface methyl bromide mole fraction are available for comparison to model results. Irregular flask measurements of methyl bromide are available at Trinidad Head, California, USA and Cape Grim, Tasmania, Australia [Miller, 1998]. In addition, a gas chromatograph-mass spectrometer (GC-MS) instrument installed at Mace Head, Ireland provides an *in situ* record of CH_3Br mole fractions dating from April 1995 [Simmonds *et al.*, 1998; P. Simmonds and S. O'Doherty, U. of Bristol, unpublished data], with sampling frequencies of four to six per day.

Flask-sampled data from California and Tasmania are discussed by Miller [1998]. The collection methodology is designed to insure that measurements are representative of "baseline," *i.e.*, remote tropospheric, abundance. Because only a few data points are available in any particular year, we consider only the climatological, monthly mean mole fractions. For comparison, six-hourly MATCH outputs outside the 95% confidence interval of the monthly mean mole fractions are excluded to eliminate data strongly influenced by local pollution sources. The effect of filtering on mean mole fraction is negligible in Tasmania, but large (and negative) at the California site, which is proximal to a large regional methyl bromide source. For comparisons between MATCH results and Mace Head observations, the same filtering process is performed on the *in situ* Irish GC-MS record. In addition, the Mace Head data is corrected to the Scripps Institution of Oceanography CH_3Br scale (SIO93) based on the intercalibration studies of Miller [1998].

Figures 5.1 through **5.4** and **Tables 5.3** and **5.4** compare modeled and observed mole fractions in Ireland, California, and Tasmania. Post-1991 observational data at Cape Grim are underestimated by 4 to 14%. Runs with higher technological sources (MLH, HMH) poorly simulate observations. Runs VEG and HLM estimate mean values somewhat more accurately. Seasonal variability is low in both modeled and observed data, but maximum modeled mole fraction is roughly six months out-of-phase with observations. At Trinidad Head, comparison of the model and observations is hindered by the limited number of measurements available, and the proximity to the large methyl bromide source from California's agricultural regions. In an attempt to minimize the impact of low model resolution, Trinidad Head observations are compared with a model grid point immediately off the coast of California. This is consistent with the sampling procedures outlined in Miller [1998], which are intended to insure that samples contain remote tropospheric air. Annual mean model-to-observed mole fraction ratios range from

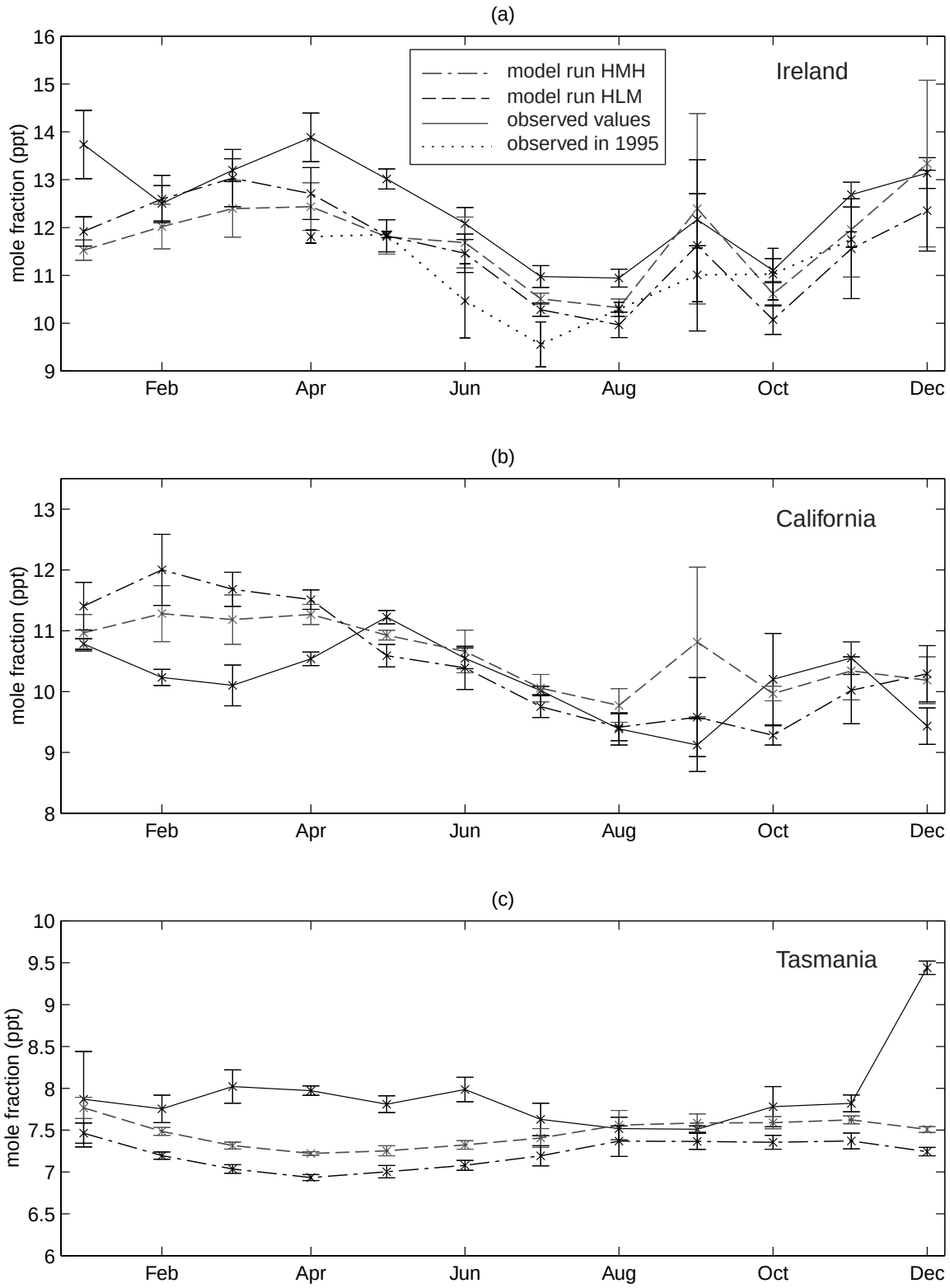

Figure 5.1. Modeled and observed monthly-averaged mole fractions. (a) At Mace Head, Ireland. (b) At Trinidad Head, California. (c) At Cape Grim, Tasmania. Solid line, observed values; dot-dashed line, run HMH; dashed line, model run HLM; dotted line inludes measurements from 1995 only. Error bars are ± one standard deviation. Model and in situ data are filtered at the 95% conficence interval to remove the effect of local pollution sources.

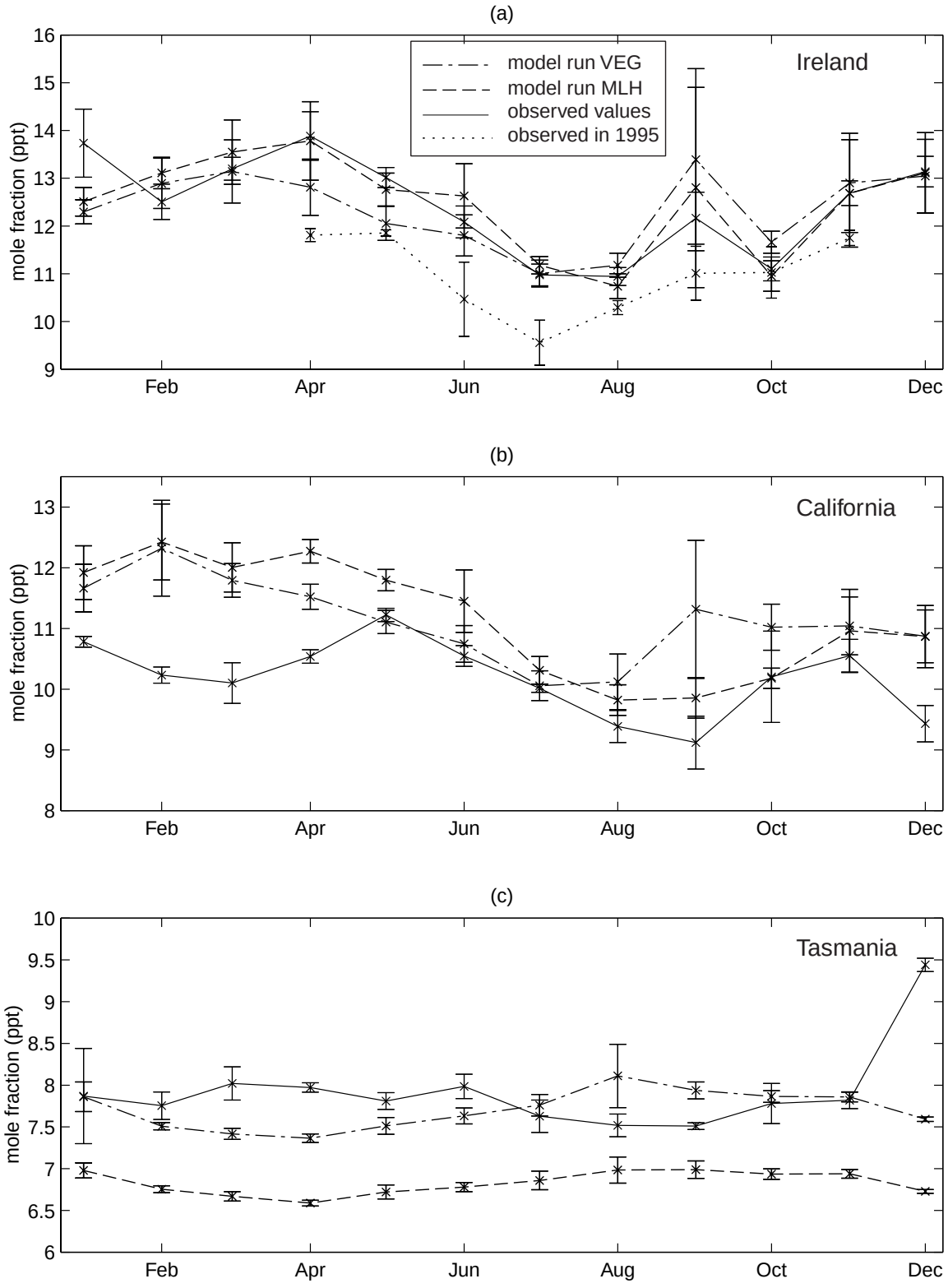

Figure 5.2. Same as Fig. 5.1. Dashed line, model run MLH; dot-dashed line, run VEG.

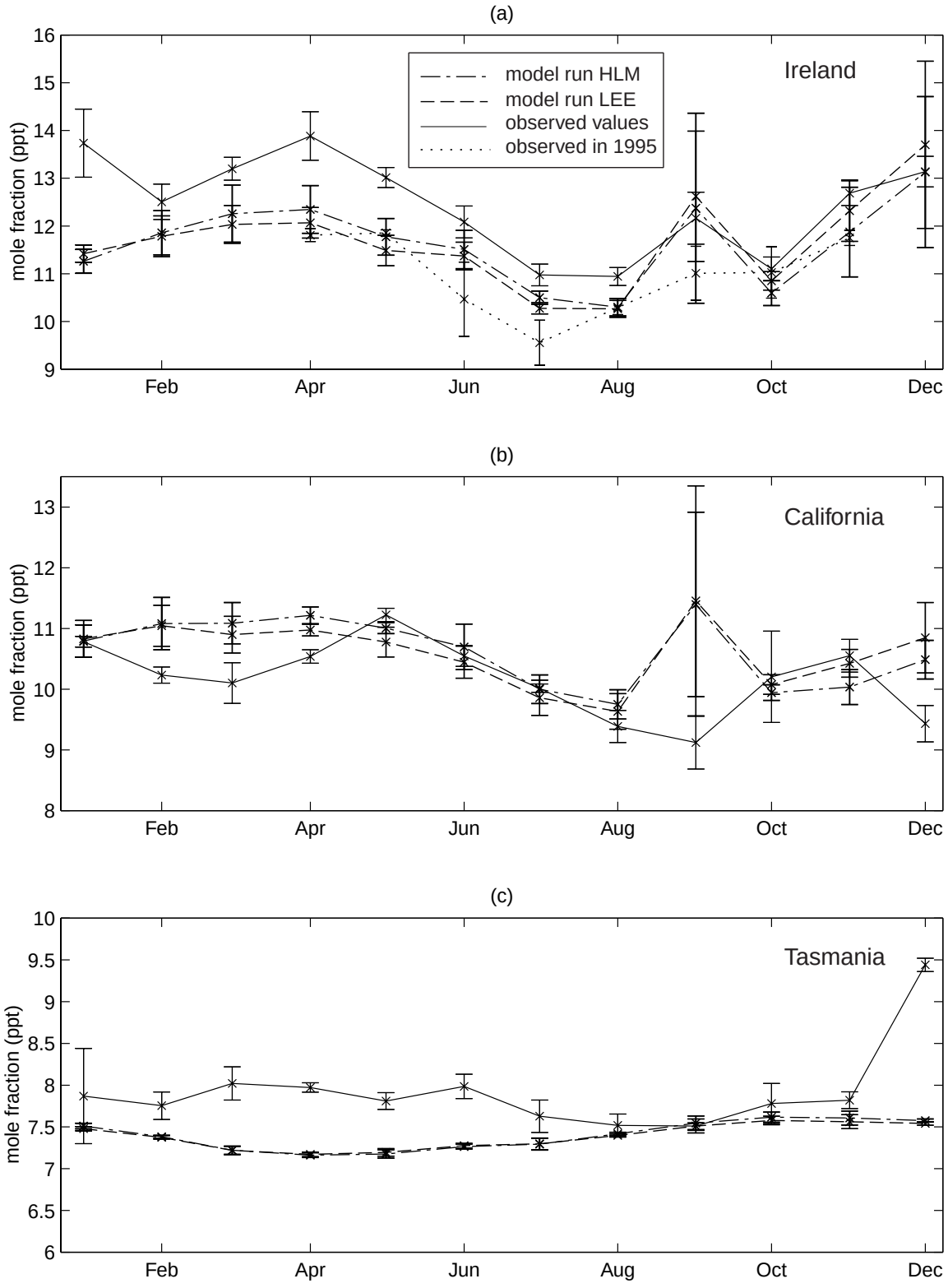

Figure 5.3. Same as Fig. 5.1. Dashed line, model run LEE; dot-dashed line, run HLM.

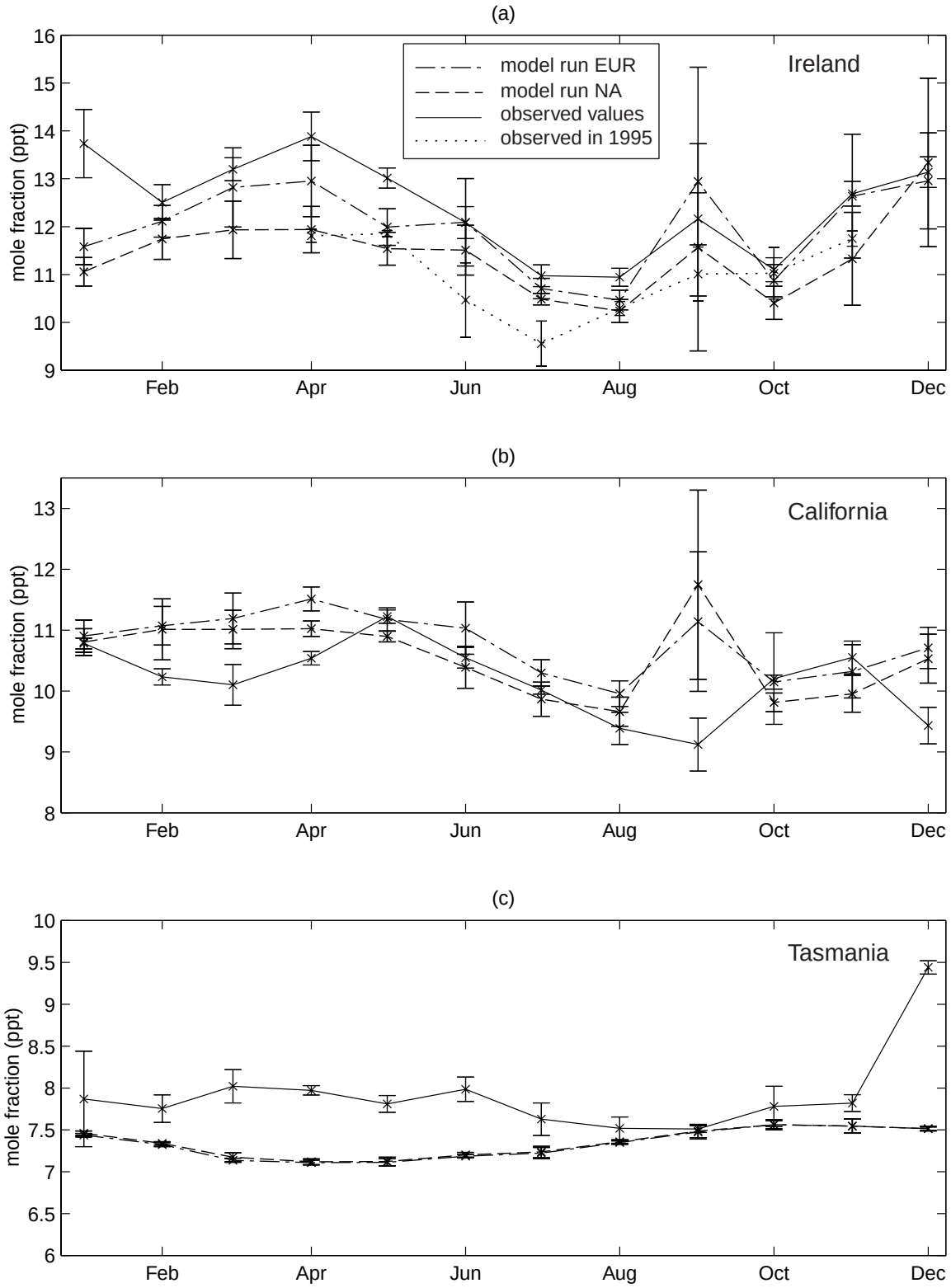

Figure 5.4. Same as Fig. 5.1. Dashed line, model run NA; dot-dashed line, run EUR.

Table 5.3. Annual Mean Modeled and Observed Mole Fraction (ppt)*

	Mace Head	Trinidad Head	Cape Grim
HLM	11.8	10.6	7.5
HMH	11.6	10.5	7.2
MLH	12.5	11.2	6.8
VEG	12.3	11.1	7.7
NA	11.4	10.6	7.3
EUR	12.0	10.8	7.3
LEE	11.7	10.6	7.4
XMM	10.8	9.9	7.5
XML	10.3	9.6	7.7
XHM	10.2	9.4	7.7
Observed	*12.5*	*10.2*	*7.9*

* Data filtered at 95% confidence interval to remove influence of local pollution. Observed data are climatological means.

Table 5.4. Root Mean Square Error of MATCH Monthly Mean Values (ppt)*

	Mace Head	Trinidad Head	Cape Grim	MH 1995 only
HLM	0.94	0.73	0.69	0.76
HMH	1.14	0.90	0.90	0.55
MLH	0.59	1.18	1.25	1.21
VEG	0.76	1.21	0.66	1.07
NA	1.25	0.94	0.76	0.62
EUR	0.73	0.87	0.76	0.94
LEE	1.35	0.87	0.73	0.80
XMM	1.84	0.97	0.62	0.76
XML	2.36	1.21	0.55	1.04
XHM	2.42	1.35	0.52	1.14

* Data filtered at 95% confidence interval; comparison to climatological observations, unless otherwise noted.

1.02 to 1.09. Cases HMH and HLM (high biomass emissions scenarios) most closely reproduce annual mean observations. Seasonal cycles are broadly consistent with oxidation by the OH radical, although model runs do not reproduce low observed mole fractions in February, March, and April.

Mole fractions in Ireland are also sensitive to European regional sources, although transport from continental Europe and the UK is fairly well resolved by the T42 grid. “Baseline” observations at Mace Head are characterized by a large seasonal cycle, with a late winter/early spring maximum that is consistent with changes in tropospheric OH and/or the activation of a large temperate soil sink during the growing season. However, the magnitude and timing of the maximum are subject to considerable interannual variability [P. Simmonds and S. O’Doherty, U. of Bristol, unpublished data]. Also, “baseline” concentrations are 10 to 30% higher than those reported at Trinidad Head. Annual mean model-to-observed mole fraction ratios range from 0.95 to 1.02 with observations adjusted to the SIO93 scale (see Miller [1998]). Scenarios HLM and HMH tend to underestimate mean mole fractions slightly. Cases VEG and MLH fall within one standard deviation of observed monthly means for most months. When only measurements from 1995 are included, the observed mole fraction is significantly lower, and runs HLM and HMH fit observed data better than cases with lower biomass burning emissions. However, significant overestimates occur in two out of eight months for which data are available. All simulations qualitatively reproduce observed seasonal variability.

The use of a three-dimensional CTM also allows comparison with high frequency *in situ* observations at Mace Head. Measurements at Mace Head are available from April 1995 to December 1995. Daily average values for model results and observations are shown in **Figure 5.5**. Model-to-observation correlation coefficients are similar for all model runs and range from 0.40 to 0.43. This compares to values of approximately 0.8 at Mace Head for the CFC-11 simulations of Mahowald *et al.* [1997a]. The difference presumably reflects the relatively poor understanding of the regional- and local-scale methyl bromide budgets.

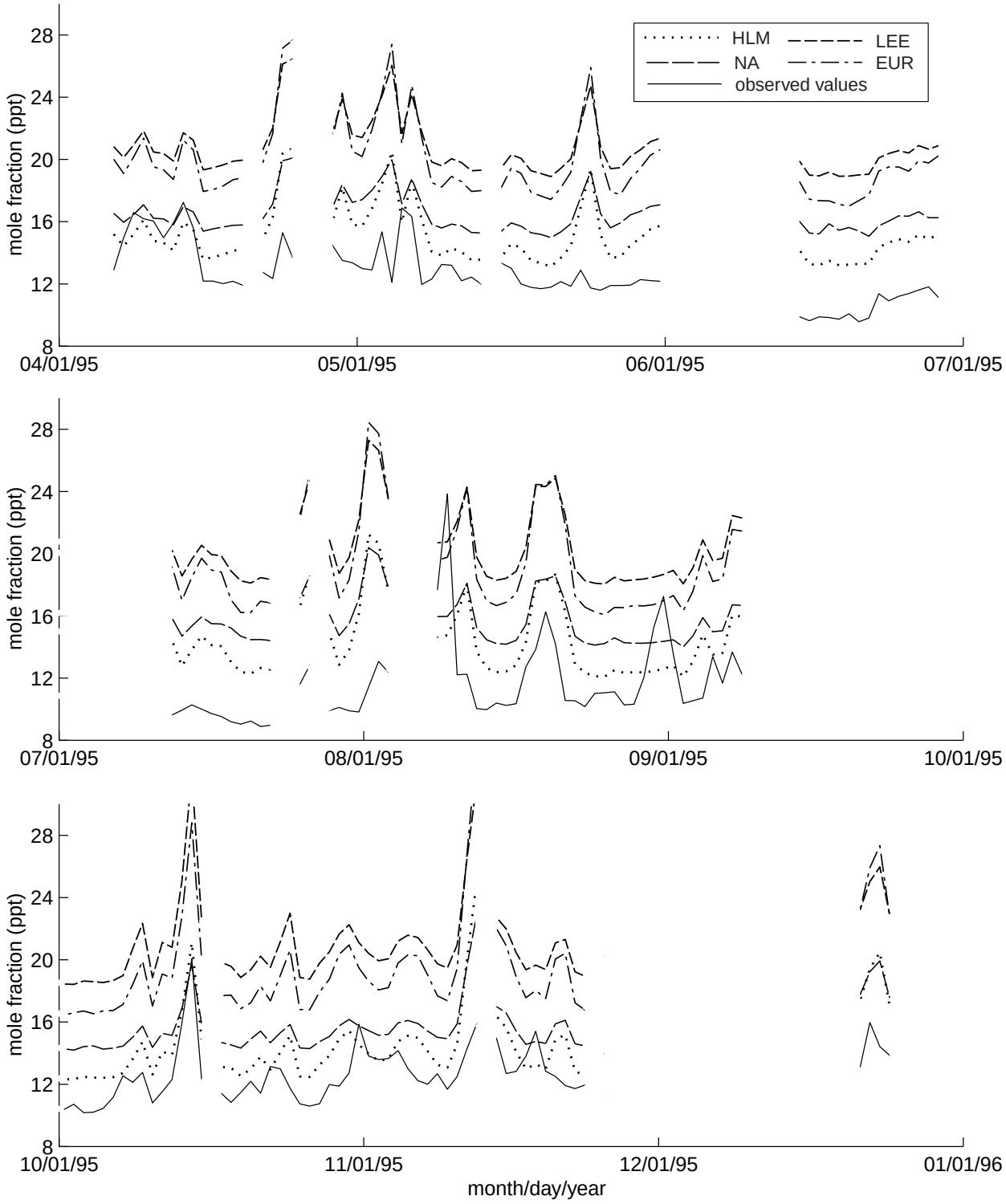

Figure 5.5. Daily average mole fractions at Mace Head, Ireland. Solid line, observed values; dotted line, model run HLM (offset 2 ppt for clarity); long-dashed line, run NA (offset 4 ppt); dot-dashed line, run EUR (offset 6 ppt); short-dashed line, run LEE (offset 8 ppt).

In the vicinity of Mace Head, high frequency variability is primarily driven by synoptic meteorology. The site is exposed to relatively low ambient mole fractions during periods of westerly winds. Winds from easterly sectors advect heavily polluted air masses from the British Isles and continental Europe. Local Irish sources, such as the burning of peat for fuel and emission from peat bogs, are also suspected of influencing observed mole fractions [P. Simmonds, U. of Bristol, personal communication]. In the model runs, it was found the timing and magnitude of pollution events is determined primarily by the distribution of industrial emissions. Model runs with high European sources (EUR) tend to overestimate the variance of daily mean mole fraction. Those with lower European sources and higher North American sources (NA) tend to underestimate the variance. Run HLM, used as a reference for the high and low emissions scenarios, predicts the variance within 3%. However, correlation coefficients for all runs are similar, and low (around 0.4), and none of the runs successfully simulates low mole fractions observed in summer 1995 (see **Figure 5.6**) More accurate results will likely depend upon a more detailed approach to the industrial source distribution within Europe, and perhaps upon better quantification of local sources in Ireland.

All model runs underestimate the quasi-zonal gradient between Trinidad Head (124˚W) and Mace Head (10˚W). The reasons for the discrepancy are unclear. Observed mole fractions at Trinidad Head are in the lower range of reported values for Northern Hemisphere mid-latitudes, while those at Mace Head exceed all recent (post-1992) long-term measurements. Possible explanations include the contamination of the Mace Head record by local sources. In addition, the collection of flask samples at Trinidad Head may be biased toward periods of abnormally low mole fraction due to meteorological criteria used to determine sampling periods. Another complication is introduced by the inability of the T42 grid to resolve advection from local sources in California. This problem is addressed by comparing measurements with modeled mole fractions from the grid point immediately west of the Trinidad Head station, but this is at best a stopgap solution. An additional source of error is the sparse observational record, which allows only a climatological comparison of modeled and measured mole fractions.

The sensitivity of the monthly mean Trinidad Head-to-Mace Head gradient to different industrial source distributions is shown in Fig. 5.6 (b). Comparison between modeled and observed results is somewhat better when only 1995 data from Mace Head is considered (measurements at Trinidad Head are not available in 1995). Climatological data suggests a much steeper zonal gradient. It is unclear if this is due to changes in methyl bromide surface fluxes, interannual meteorological variability, or bias due to gaps in the instrumental record, which could be quite large due to infrequent observations in California. Mace Head mole fractions show greatest sensitivity to changes in the spatial pattern of industrial emissions. Annually averaged values (of monthly means filtered at the 95% confidence interval) increase 3.1% if Eurasian emissions increase by 10 Gg y^{-1} (run EUR), and decrease by 1.8% for higher North American emissions balanced by lower Eurasian emissions (run NA). Interestingly, baseline mole fractions at Trinidad Head show virtually no sensitivity to elevated North American emissions (–0.6%), and small but positive sensitivity to increased Eurasian emissions (1.6%).

Both sites show a similar response to the monthly soil fumigation emissions distribution of Lee-Taylor *et al.* [1998] (run LEE). The largest deviations from reference mole fractions occur in the boreal autumn (see Fig. 5.3), coinciding with the annual peak in fumigation emissions.

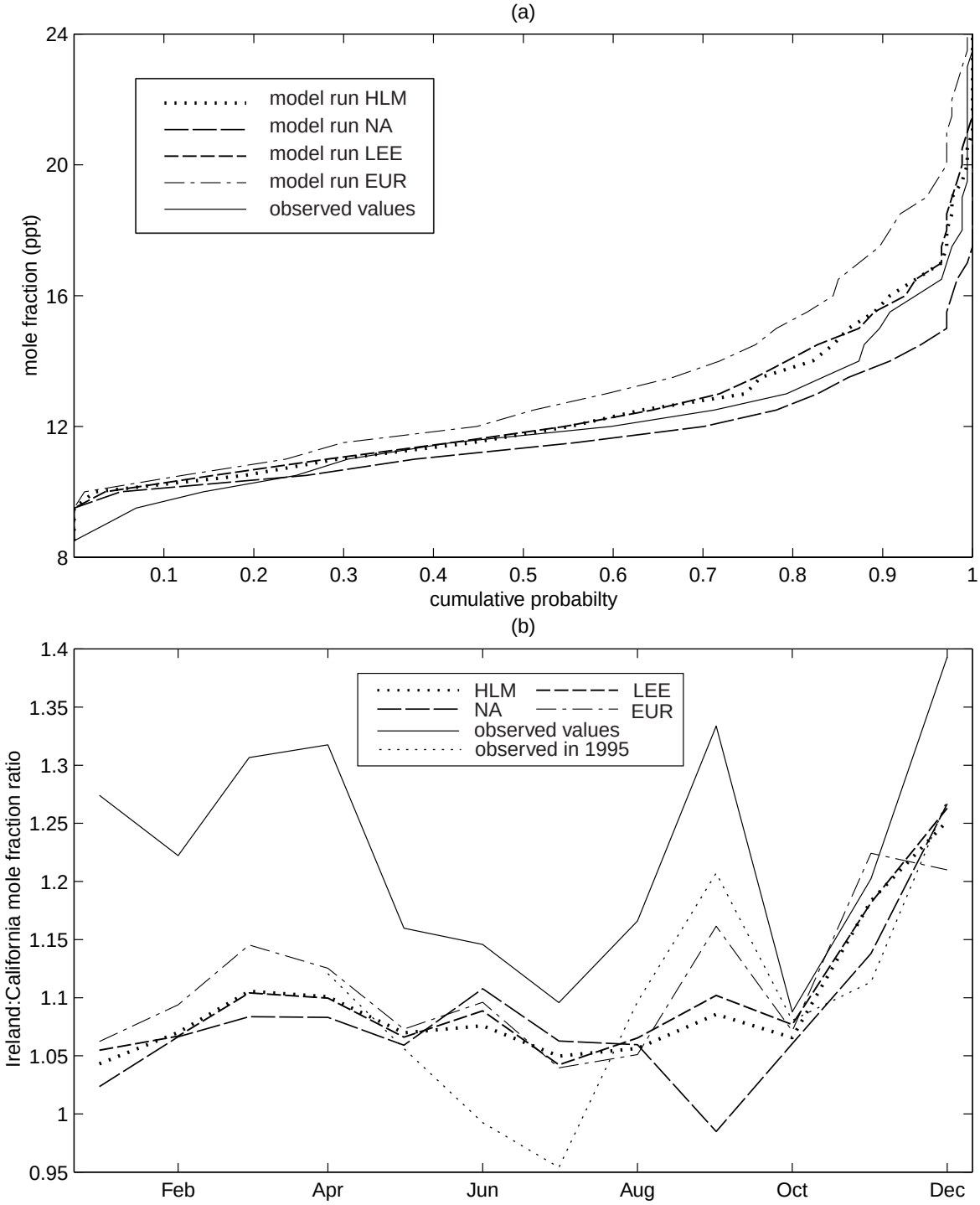

Figure 5.6. (a) Probablity distributions for measured and modeled daily average concentrations at Mace Head, Ireland, April–December, 1995. Statistics include only periods in which obserational and model data overlap. (b) Ratio of surface mole fractions at Mace Head, Ireland and Tinidad Head, California. Values are monthly mean data filtered at the 95% confidence interval. The thin dotted line includes Mace Head data from the year of the model run (1995) only. Solid line, observations; thick dotted line, model run HLM; long-dashed line, run NA; dot-dashed line, run EUR; short-dashed line, run LEE.

Maximum change in monthly mean mole fraction is 4.4% at Mace Head and 3.9% at Trinidad Head. Surface concentrations in the Southern Hemisphere are virtually identical in model runs NA, EUR, and LEE.

5.2 Additional Measurements

Additional published atmospheric measurements of CH_3Br include the flask-sampled time series of Cicerone *et al.* [1988] and Khalil *et al.* [1993], the *in situ* measurements of Lobert *et al.* [1995, 1996, 1997], and the intensive campaigns in Alaska and New Zealand described by Wingenter *et al.* [1998] and Blake *et al.* [1996]. These data, along with the Miller [1998] measurements and Mace Head GC-MS time series [P. Simmonds and S. O'Doherty, pers. comm.], provide an estimate of the climatological range of methyl bromide concentrations. Seasonally averaged observations are compared with seasonally-zonally averaged model mole fraction in **Figure 5.7**. Note that model results exclude data from non-Antarctic grid cells over land to reflect the bias of observations toward coastal and marine locations. For boreal winter, spring, and summer data, MATCH overestimates the meridional gradient, with interhemispheric ratio (IHR) exceeding the area and variance weighted measured values by 10 to 40%. Scenarios containing higher technological sources (HMH and MLH) tend to deviate most widely from observations, while runs VEG and HLM agree most closely with observed surface mole fraction. In contrast, all scenarios, save MLH, slightly underestimate the meridional gradient in the boreal autumn (September–November).

Deviations from observed values are largest in the December–February period, with modeled mole fraction significantly exceeding measured values in the Northern Hemisphere, and the ratio is reversed at mid-latitudes in the Southern Hemisphere. Observations at Mace Head, Ireland [P. Simmonds and S. O'Doherty, U. of Bristol, unpublished data] are notable exceptions. Overall, the balance of observations implies that Northern Hemisphere fluxes used in the "balanced" MATCH runs are estimated to be too high in the boreal winter, and that Southern Hemisphere fluxes are simultaneously underestimated. The seasonal variability of soil fumigation emissions proposed by Lee-Taylor *et al.* [1998] implies higher emissions in the boreal fall, and lower emissions in the boreal winter and summer. Model simulations (run LEE) indicate the maximum monthly calculated IHR is 2% lower using the Lee-Taylor soil fumigation parameterization, and the minimum monthly IHR is 3% higher. The IHR in the boreal winter and spring still significantly exceeds measured values in run LEE. Nonetheless, observations are consistent with a smaller soil fumigation flux in the boreal winter. It is also possible that biomass burning emissions in the Southern Hemisphere may be underestimated during the Austral summer.

In general, the role of soil surface sinks is difficult to disentangle from technological emissions due to their similar meridional distributions. A reduced soil sink does in some cases lead to better agreement with data at high Northern latitudes, as is the case at Mace Head, Ireland. However, measurements from California [Miller, 1998] and Alaska [Cicerone *et al.*, 1988; Wingenter *et al.*, 1998] are inconclusive on this count. On the other hand, the heavy weighting of the soil sink toward the Northern Hemisphere implies a larger sink would be consistent with the observed interhemispheric ratio. However, the discrepancy between modeled and observed IHR is most pronounced in boreal winter, when the soil microbial activity in the Northern Hemisphere is at a minimum. Increased soil deposition would most strongly impact mole fractions during the boreal summer and fall, periods in which MATCH simulates meridional gradients relatively well.

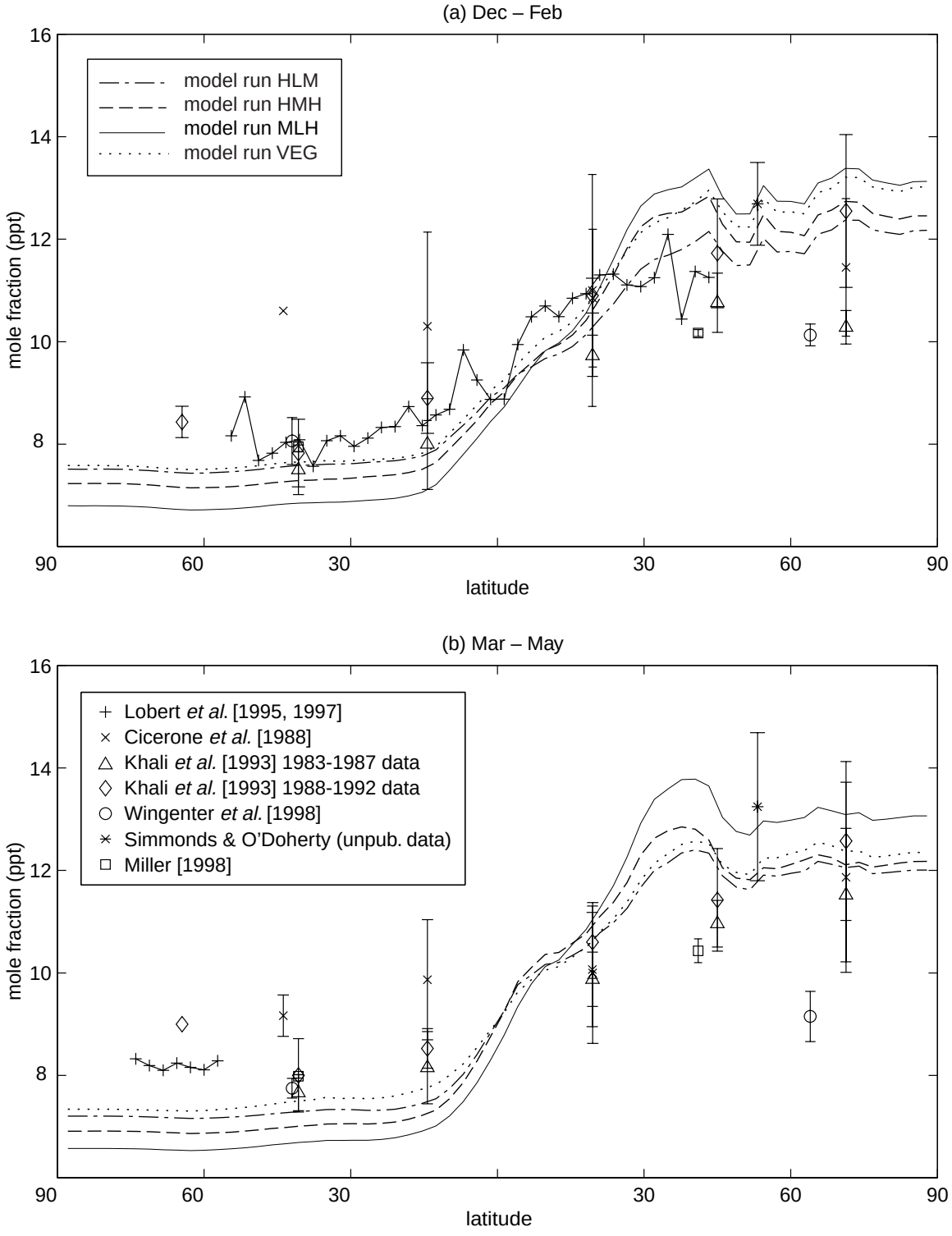

Figure 5.7. Observed and modeled surface model fractions. Lines are zonally averaged model output from grid cells over oceans and Antarctica. (a) Dec–Feb average. (b) March–May. Dot-dashed line, model run HLM; dashed line, run HMH; solid line, run MLH, dotted line, run VEG. Observations are: '+', Lobert *et al*. [1995, 1997]; 'x', Cicerone *et al*. [1998]; '△', Khalil *et al*. [1993], 1983–1987 data; '◇', Khalil *et al*. [1993], 1988–1992 data; 'O', Wingenter *et al*. [1998]; '*', P. Simmonds and S. O'Doherty [unpublished data]; and '□', Miller [1998]. (continued…)

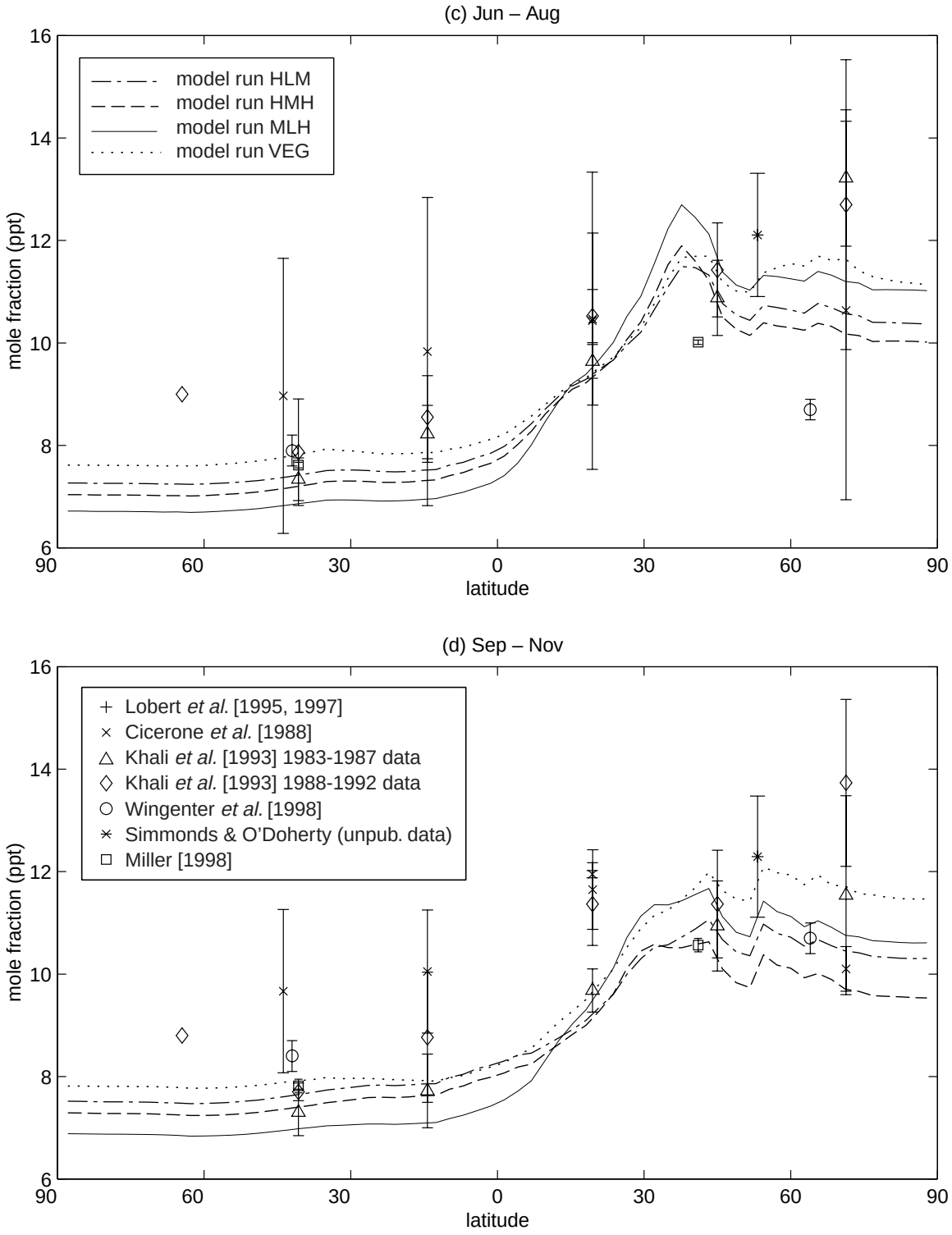

Figure 5.7 (continued). Observed and modeled surface model fractions. Lines are zonally averaged model output from grid cells over oceans and Antarctica. (c) June–Aug. (d) Sep–Nov. Note that the Lobert *et al*. [1995, 1997], Miller [1998] and Simmonds/O'Doherty data are calibrated against the SIO93 scale based on the intercalibration studies of Miller [1998].

5.3 Investigations into the Possibility of an Enhanced Biomass Burning Source

Results from the "balanced" MATCH runs indicate that the current understanding of the methyl bromide budget is incompatible with existing atmospheric measurements. Observed meridional gradients and interhemispheric ratios are overestimated by 10 to 40% in the balanced model runs. However, model runs with higher biomass burning sources (HLM and HMH) better simulate observed IHR due to the fact that biomass fire emissions are relatively evenly distributed between the hemispheres (at a roughly 3:2 Northern Hemisphere-to-Southern Hemisphere ratio). In an attempt to reproduce IHRs within the range of observed values, several additional scenarios are constructed with an annual biomass burning flux in excess of the 50 Gg y^{-1} maximum used in the "balanced" model runs. Global mass balanced is maintained by simultaneously reducing the magnitude of soil fumigation emissions and/or increasing the soil sink (see Table 4.1).

"High biomass burning" run results are summarized in **Table 5.5**. Interhemispheric ratios vary from 1.21 to 1.29, within the range of observations by Wingenter *et al.* [1998] and Lobert *et al.* [1995] (see also Miller [1998]). While total atmospheric burden for the high biomass burning scenarios falls within the range established by the balanced runs, global mean surface mole fraction is slightly lower. This can be attributed to the increased magnitude of low-latitude sources in the high biomass burning runs, which facilitates rapid vertical mixing *via* the ascending branch of the Hadley circulation.

Comparison with time series and seasonally-zonally averaged observations yields mixed results (see **Figures 5.8** and **5.9**). When compared with the balanced runs, high biomass burning runs better simulate observed abundance during the boreal winter. Again, Irish observations are an exception to this rule. Climatological, annual mean mole fractions at Mace Head are 1.7 to 2.3 ppt higher than model runs XMM, XML, and XHM, although the fit is significantly better when only data from the year of the model run (1995) are considered. During the boreal summer and autumn, runs XMM, XML, and XHM all underestimate meridional gradients. Northern Hemisphere mole fractions are significantly underestimated during the September–November period. The model may also underpredict mole fractions in Northern Hemisphere mid-latitudes during June–August, but the wide range of observed values prohibits any definitive statement on this matter.

Table 5.5. Results from High Biomass Burning MATCH Runs*

	XMM	XML	XHM
Atmospheric burden (Gg)	132	131	132
Mean surface mole fraction (ppt)	9.1	9.0	9.0
Surface interhemispheric ratio	1.29	1.21	1.21

* Annual average global values.

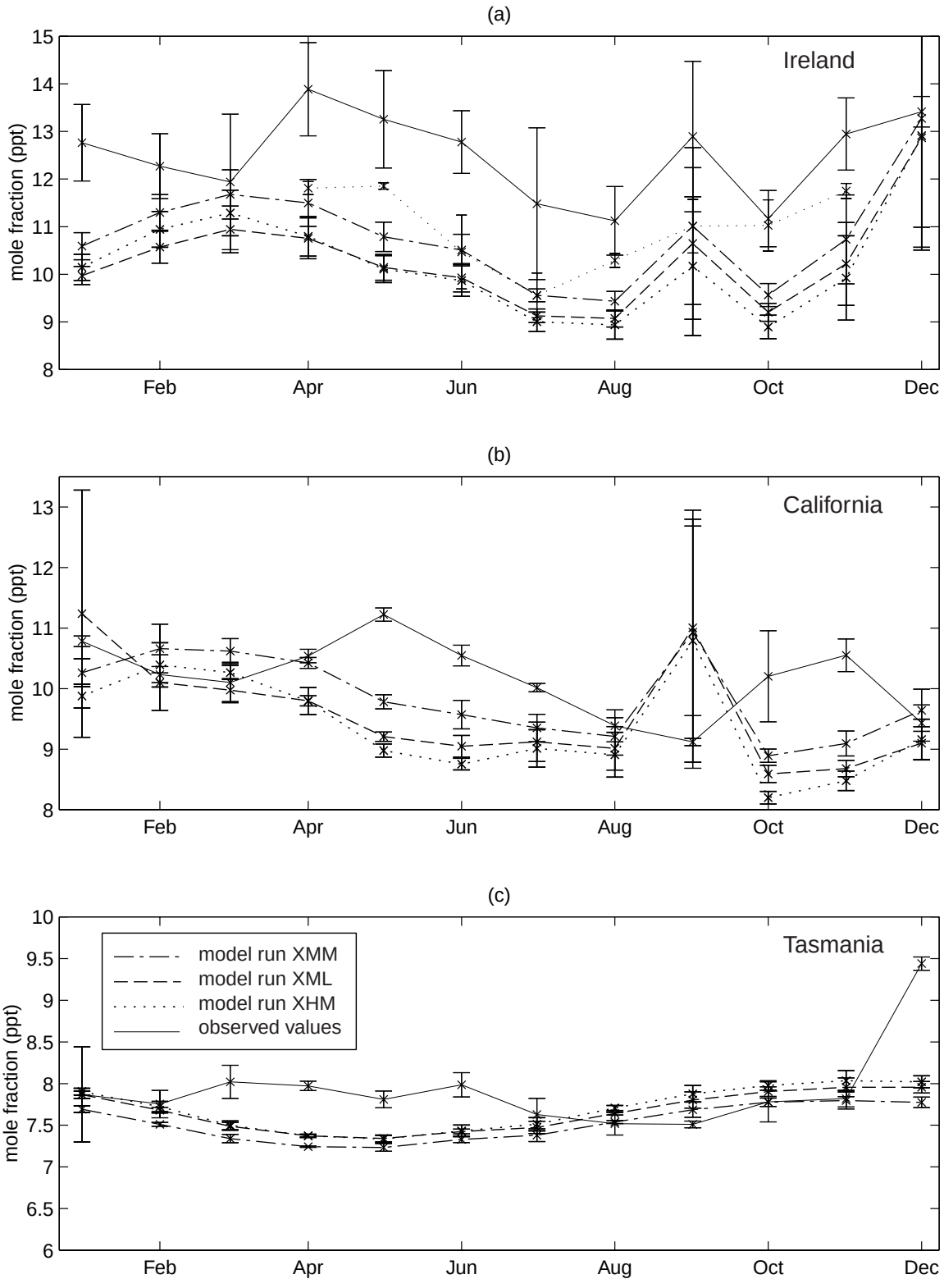

Figure 5.8. Same as Fig. 5.1. Dashed line, model run XML; dot-dashed line, run XMM; dotted line, run XHM.

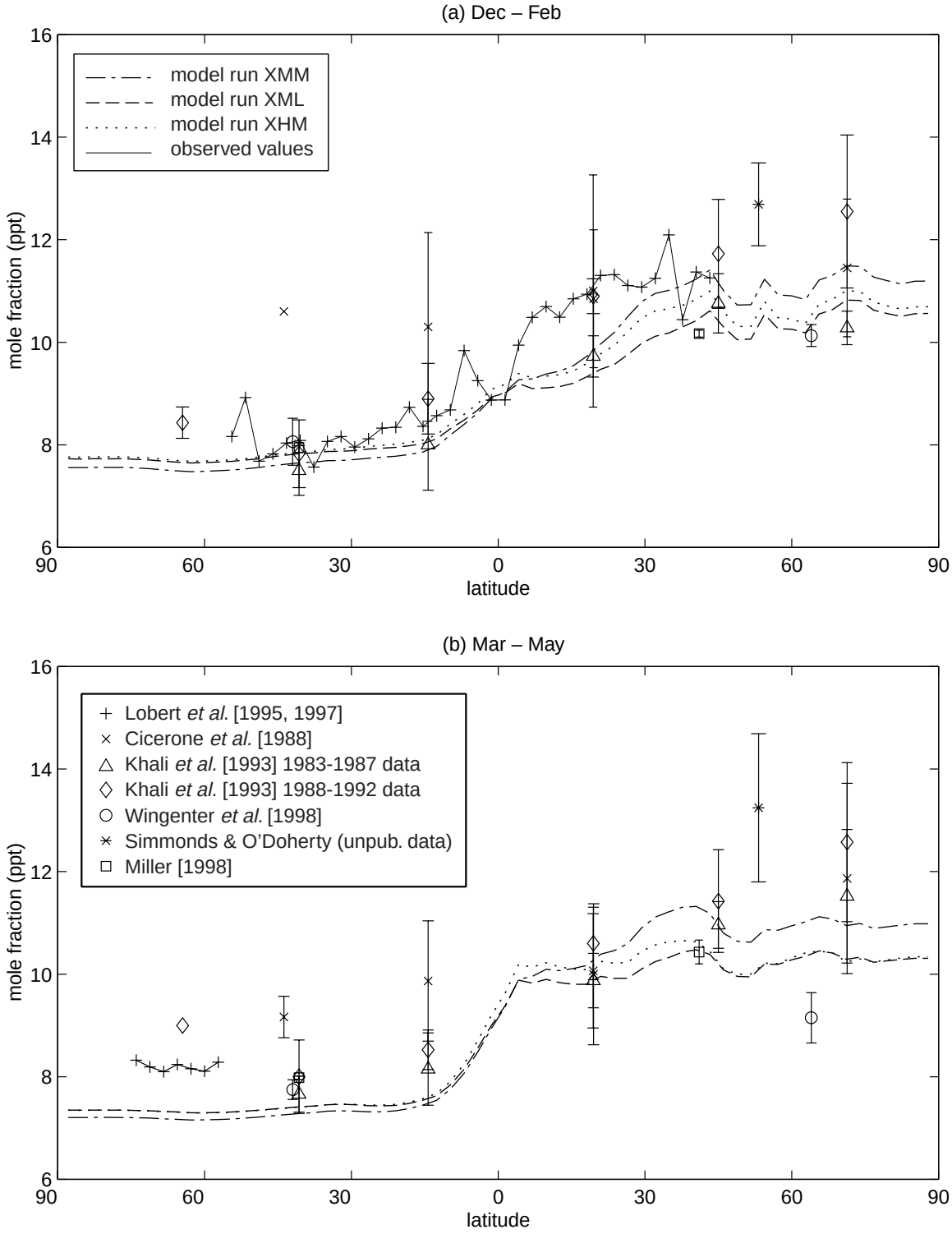

Figure 5.9. Comparison of observed surface mole fractions with "high biomass burning" model runs. Lines are zonally averaged model output from grid cells over oceans and Antarctica. Dashed line, run XML; dot-dashed line, run XMM; dotted line, run XHM. (a) Dec–Feb average. (b) March–May. (continued…)

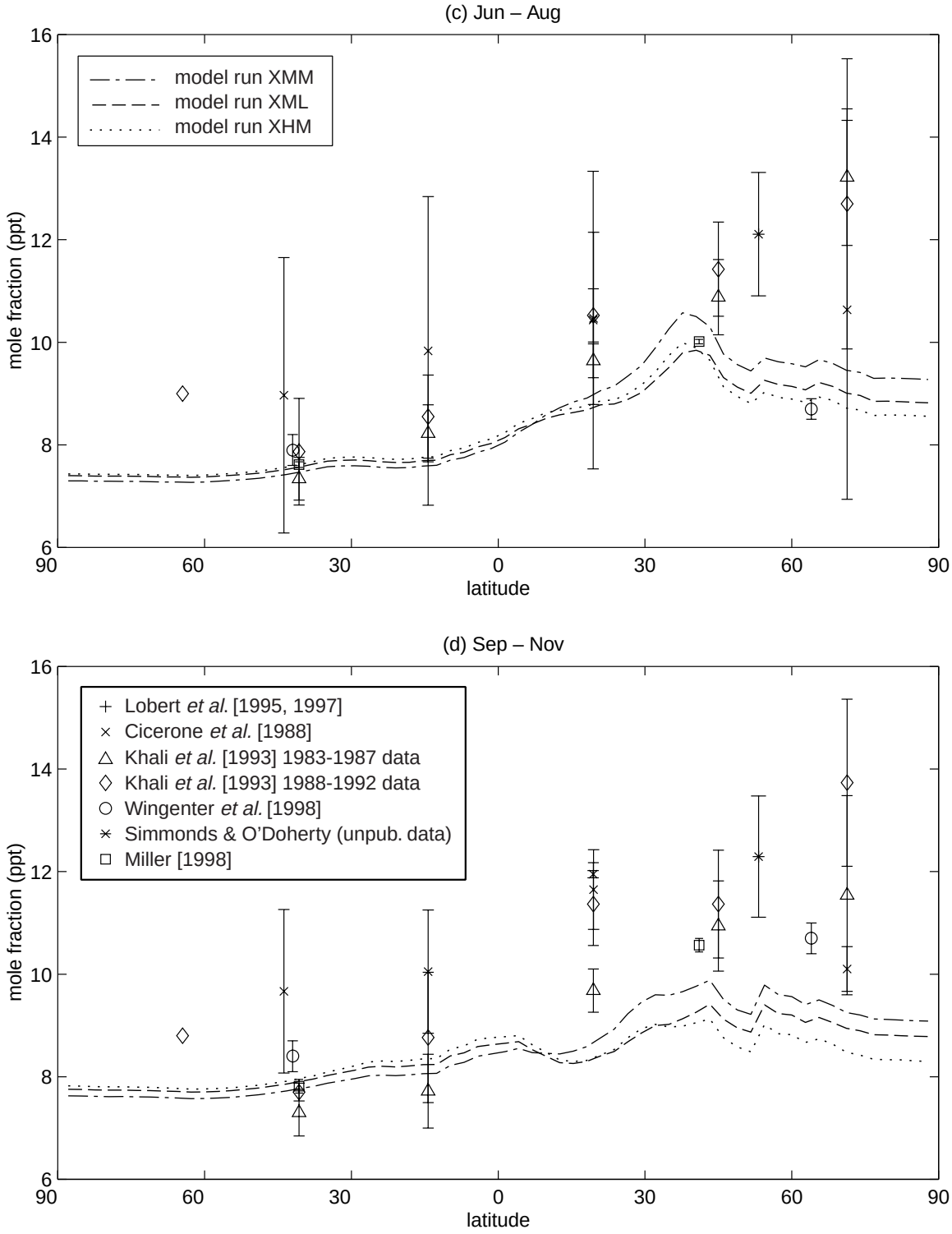

Figure 5.9 (continued). Comparison of observed surface mole fractions with "high biomass burning" model runs. Lines are zonally averaged model output from grid cells over oceans and Antarctica. (c) June–Aug. (d) Sep–Nov. Dashed line, run XML; dot-dashed line, run XMM; dotted line, run XHM. Observations are as in Fig. 5.7. Note that the Lobert *et al*. [1995, 1997], Miller [1998] and Simmonds/O'Doherty data are calibrated against the SIO93 scale based on the intercalibration studies of Miller [1998].

The same seasonal pattern of over- and underestimation, six months out-of-phase, is apparent in the Cape Grim time series. With the exception of the anomalously high measured mole fraction in December, annual mean values are simulated quite accurately by the high biomass burning runs (within 0.1–0.3 ppt). However, predicted mole fractions are too high in the Austral winter and too low in the Austral summer. Modeled abundance is qualitatively consistent with the seasonal cycle of tropospheric OH at Southern mid-latitudes. Observations show little seasonal variability, suggesting the influence of an unidentified flux with a seasonal cycle peaking in the Austral summer. Biomass burning flux to the Southern Hemisphere is highest in September and October, coinciding with the dry season in the seasonally humid tropics. Therefore, higher tropical biomass burning emissions are unlikely to account for the observed absence of a summer minimum in the Cape Grim time series. Regardless, the effect of biomass burning emissions on modeled mole fractions in the extratropical Southern Hemisphere is small relative to tropical continental regions.

5.4 Sensitivity to Surface Fluxes

The balanced MATCH runs are used to compute the sensitivity of surface methyl bromide mole fractions to biomass burning flux, soil fumigation emissions, and soil deposition velocity. In addition, the sensitivity to a hypothetical vegetation source (run VEG) is considered. We define sensitivity of the mole fraction χ_i at position i to the change in flux ΔF_j from source j as

$$H_{ij} = \Delta F_j^{ref} \frac{\Delta \ln \chi_i}{\Delta F_j}$$

where ΔF_j^{ref} is an arbitrary normalization factor, which is taken to be 25 Gg y^{-1} (a typical uncertainty of the mid-range flux estimates). Regions of high sensitivity are therefore ideal locations to site monitoring stations for the purpose of surface flux estimatation. H_{ij} also provides an estimate of the accuracy of measurements and models needed to reduce uncertain terms in the budget. Annual mean surface sensitivities are shown in **Figures 5.10** and **5.11**.

Figure 5.12 shows which flux results in the largest value of H_{ij} at each model grid point i, as well as the percentage of the total sensitivity at that grid point attributable to the primary determinant of surface mole fraction, *i.e.*

$$\frac{\max(H_{ij})}{\sum_j H_{ij}}$$

where j accounts for biomass burning emissions, soil sinks, soil fumigation fluxes, and a hypothetical source from terrestrial vegetation (model run VEG). Among known sources, sensitivities to soil deposition fluxes and technological sources are largest at Northern Hemisphere mid-latitudes. Conversely, biomass burning sources are of primary importance in tropical continental areas, and are relatively important in the Southern Hemisphere as a whole. A hypothetical source from vegetation shows a more globally uniform sensitivity (based on a source of 25 Gg y^{-1}), but is also relatively important in the Southern Hemisphere due to the smaller total source strength there.

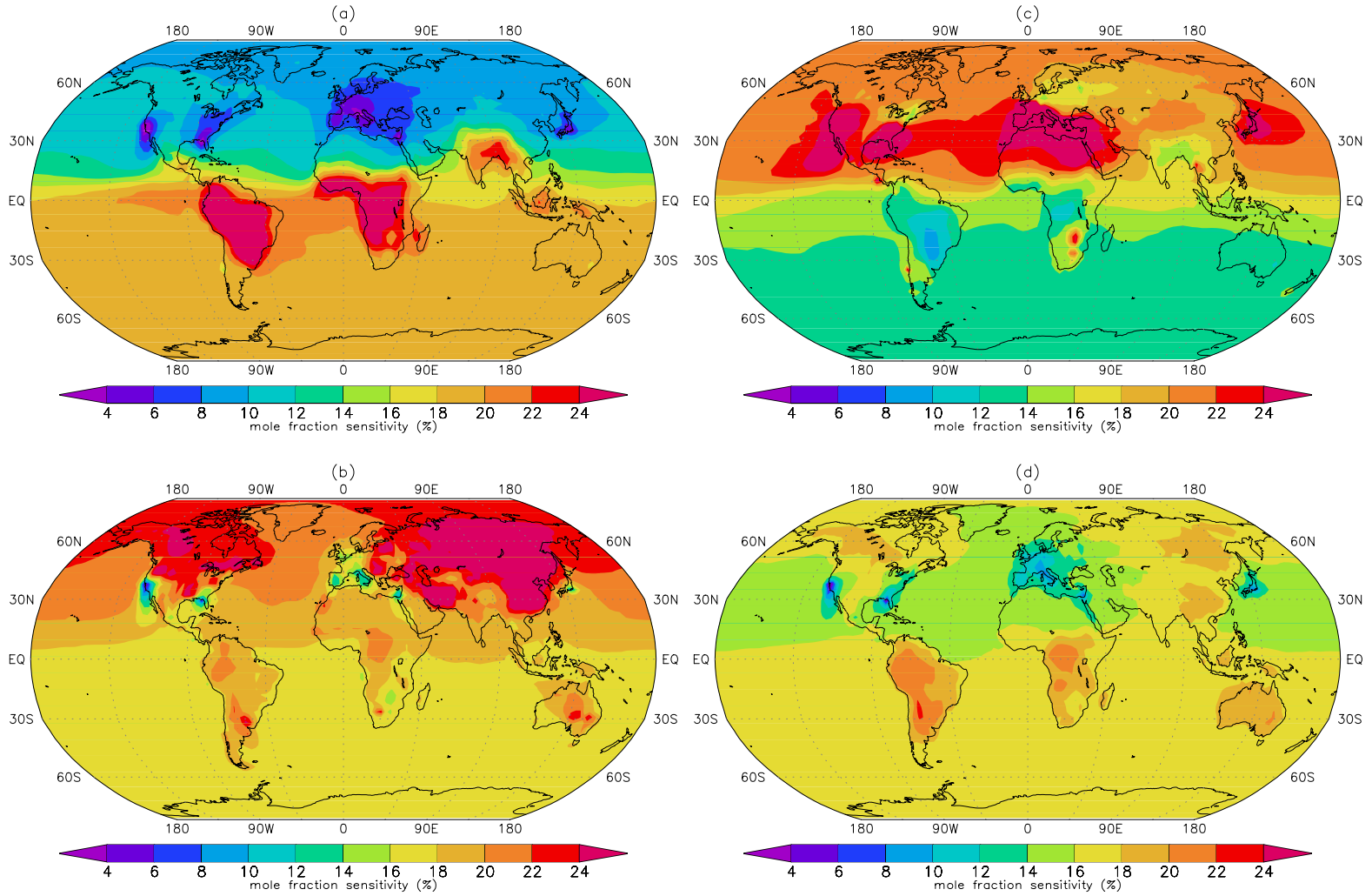

Figure 5.10. Annual average percent sensitivity of surface mole fraction to model parameters. (a) Sensitivity to 25 Gg y^{-1} increase in biomass burning emissions. (b) Sensitivity to 25 Gg y^{-1} decrease in soil sink. (c) Sensitivity to 25 Gg y^{-1} increase in soil fumigation emissions. (d) Sensitivity to 25 Gg y^{-1} flux from vegetation.

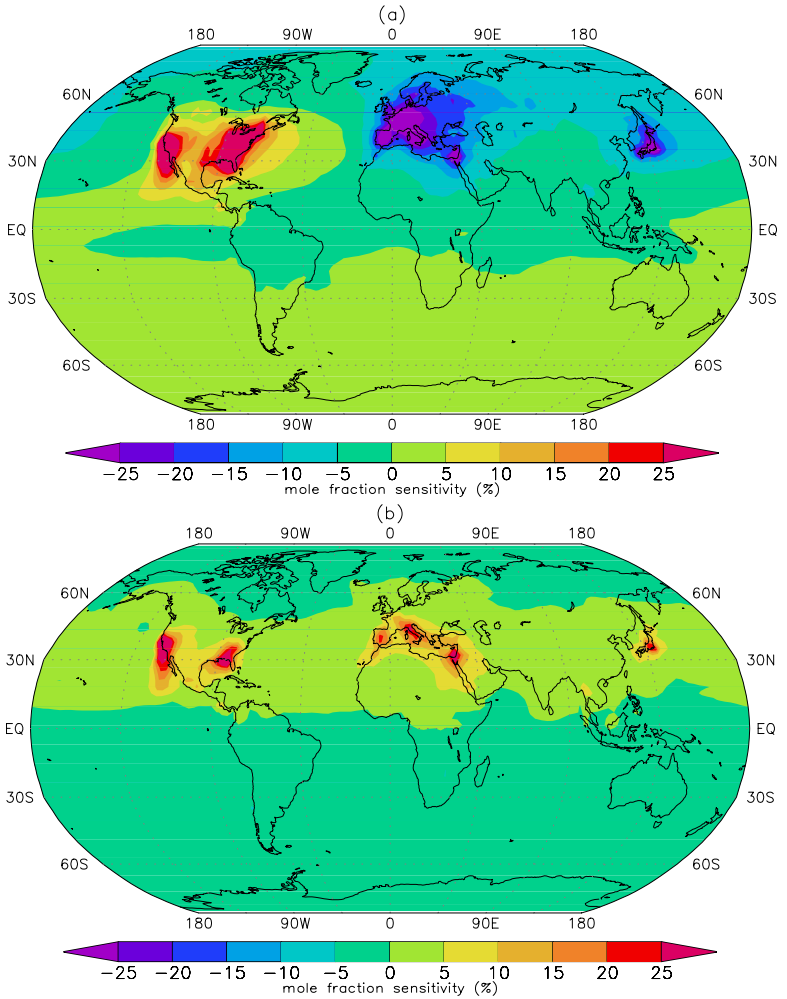

Figure 5.11. Sensitivity of surface mole fraction to distribution of techological emissions. (a) Annual mean sensitivity to increased North American source and reduced European source (percent change, run HLN minus run HLE). (b) Sensitivity to soil fumigation emissions scenario after Lee-Taylor *et al*. [1998] for month of September (percent change, run HLL minus run HLM).

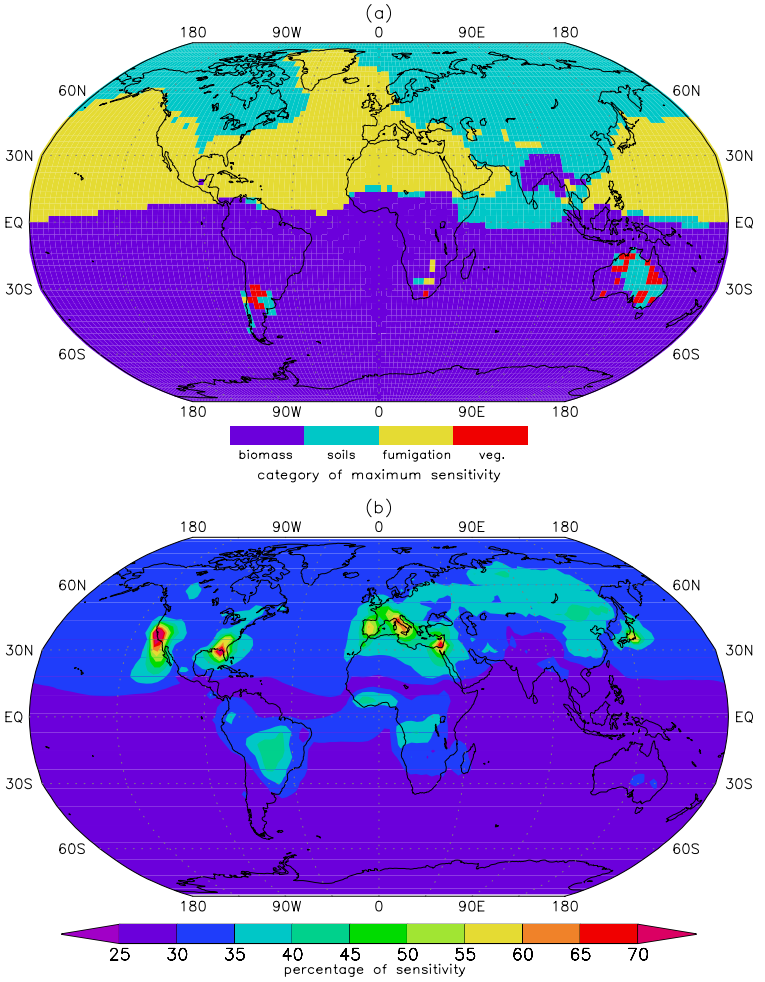

Figure 5.12. (a) Primary determinant of surface mole fraction for model grid points, as determined by largest sensitivity coefficient at grid point (see text). (b) Percentage of sensitivity at grid cell attributable to largest sensitivity coefficient from (a), *e.g.*, 25% indicates equal contribution from all four flux categories; 100% indicates surface mole fraction at grid point is determined only by the flux identified in (a).

Restricting our discussion to known sources, it is likely that accurate, long-term monitoring of the meridional gradient in the remote troposphere would provide considerable information about the importance of biomass burning emissions in the global budget. However, perhaps the most striking features of Figs. 5.10 and 5.12 are the small and similar sensitivities of extratropical Southern Hemisphere mole fractions to terrestrial sources and sinks. This speaks to the paucity of methyl bromide surface fluxes at southern mid- and high-latitudes, and demonstrates the extent to which concentrations at these latitudes are controlled by meridional transport. Surface flux estimates derived from monitoring stations in the Austral temperate regions (*e.g.*, Cape Grim) therefore depend strongly upon the accuracy of modeled advection and diffusion. In addition, limitations on observational accuracy and precision are exacerbated by the low sensitivity in these regions. Conversely, in the tropics, sensitivities to biomass burning sources are higher and less dependent upon long-range transport, particularly in continental regions and in areas where the atmospheric chemistry is subject to heavy continental influence, such as the South Atlantic. Long-term monitoring stations in one or more or these locations would likely prove invaluable to the atmospheric science community and the policy-making bodies that depend upon that community for direction and advice.

Other fluxes are less amenable to a one-dimensional, monthly-mean observational framework. Meridional distributions of soil sinks, technological sources, and leaded fuel sources (not shown) are likely to be similar. Soil sink sensitivities are highest over temperate continental regions. However, outside of Siberia, zonal gradients are relatively uniform. Longitudinal gradients of technological flux are stronger at northern mid-latitudes due to large fumigation sources in Europe, North America, and Japan. While seasonal cycles could in principle provide useful information for differentiating between the various mid-latitude sources and sinks, in practice parameters controlling the seasonal variability of fluxes are not well understood, and are likely to be highly dependent on local conditions. In addition, model results at the Mace Head and Trinidad Head locations, after removing high frequency “pollution events” from the data, indicate that even large changes in the zonal distribution of fluxes can result in relatively small changes in remote, “baseline” concentrations at mid-latitude observation sites. Background mole fraction changes on the order of a few percent, such as those due to large changes in industrial flux distribution in model runs EUR and NA, would be almost indistinguishable from noise in the baseline signal.

However, regional changes in industrial sources clearly have an impact on the magnitude of deviations from baseline values that are apparent in *in situ* records such as the Mace Head GC-MS time series (see Fig. 5.5). It is possible that regional modeling of high frequency pollution episodes could provide quantitative information about the nature and magnitude of technological sources and soil sinks [*e.g.*, Derwent *et al.*, 1998]. Ideally, high frequency instruments would be positioned downwind of large source/sink regions (*e.g.*, Europe, Japan, and North America for industrial sources, Siberia for soil sinks). Combined with regional dispersion models, a network of well-placed *in situ* instruments could significantly improve the accuracy of current flux estimates. Such an approach recognizes the spatial and temporal heterogeneity of the methyl bromide flux and concentration fields. Presently, the accuracy of such models is restricted not only by limitations of meteorological data but also the problem of assigning boundary conditions for methyl bromide mole fractions to a sub-global domain. Additional constraints are *situ*, high frequency instruments capable of quantifying CH_3Br at ambient concentrations. The success of

regional-scale modeling studies is therefore linked to improvements in the database of long-term atmospheric measurements and to the continuing refinement of global-scale simulations.

6. SUMMARY AND CONCLUSIONS

This study focused on defining and modeling the role of terrestrial surface fluxes in the global methyl bromide budget, in an attempt to simulate observed steady state atmospheric mole fractions. To account for the large deficit in the current atmospheric budget, reasonable estimates of sources and sinks were taken so as to yield steady-state surface mole fractions within the 9–10 ppt range. The resulting net surface fluxes were almost 50 Gg y^{-1} above mid-range estimates. A three-dimensional chemical transport model driven by analyzed observed winds was then used to determine the corresponding distributions of tropospheric methyl bromide.

Considering only the geographic distribution of known sources and sinks, model runs postulating a global biomass burning flux of 50 Gg y^{-1} were most consistent with observations. A hypothetical source from living vegetation also simulated zonal concentration gradients well relative to other model results. Additional simulations employing biomass burning fluxes in excess of 50 Gg y^{-1} better simulated observed, annual mean interhemispheric gradients, but underestimated mole fractions in the northern mid-latitudes, especially during the boreal autumn.

Model runs were compared to time series observations at Mace Head, Ireland, and interannually averaged measurements from Ireland, California, and Tasmania. Results from "balanced" runs were similar to monthly mean observations at Mace Head. Model runs with high technological sources underestimated observed mole fractions in Tasmania by as much as 25%, but those with larger Southern Hemispheric sources simulated annual mean abundance to within 0.3 ppt. In simulations constrained by estimated uncertainties in the surface flux budget, MATCH overestimated observed mole fraction in California. The reason for the failure to simulate the zonal gradient between California and Ireland is unclear. In addition, the model did not reproduce seasonal variability at Cape Grim, Tasmania. The persistent deficit during the Austral summer at the Tasmanian site suggests an unidentified source or local, regional, or semi-hemispheric significance.

Sensitivities of predicted surface mole fractions to different source/sink scenarios were considered. It is found that a meridionally distributed array of monitoring stations should be able to differentiate between biomass burning emissions and other known surface fluxes, especially if tropical locations are included in the network. However, other terrestrial fluxes would not be easily estimated from such a one-dimensional array of long-term monitoring stations, particularly if that network focuses primarily on deducing monthly or seasonal mean concentrations. However, high frequency variability in the CH_3Br mole fraction proved to be strongly sensitive to zonal surface flux distributions (*e.g.*, the Mace Head GC-MS time series) and could provide important constraints on zonally varying sources and sinks with similar meridional distributions and poorly characterized seasonal variability.

In light of the calculated surface mole fraction sensitivities and the demonstrated value of high frequency measurements, several deficiencies of current and possible future sites within the two major global real-time halocarbon monitoring networks, operated by the NOAA-CMDL and AGAGE organizations (see **Figure 6.1**), become apparent. Process-based models predict large

surface fluxes from the United States, Europe, the Middle East, and Japan (due to technological sources); from Northern Canada and Siberia (due to soil deposition sinks); and from tropical continental regions (due to biomass burning emissions). Mole fraction sensitivities are correspondingly large in and around these areas. The most notable features of Fig. 6.1 are the preponderance of North American locations in the monitoring networks, and the total absence of measurement capabilities in Asia, Africa, and South America. The availability of real-time measurements in these regions has been limited by the admittedly daunting task of maintaining sensitive instrumentation in remote or underdeveloped regions. Nonetheless, the implications of this study—in particular the proposal that a complete understanding of the global methyl bromide budget requires zonally-distributed, high frequency measurements of CH_3Br mole fractions—suggest that the benefits of expanding the long-term monitoring networks outside of their historical North American and maritime locations would be substantial.

The small number of long-term, contemporary observations of tropospheric CH_3Br abundance, as well as the large uncertainties in process-based estimates of surface fluxes, will limit further progress in the modeling of atmospheric methyl bromide. However, with an improved observational database, global-scale optimal estimation of methyl bromide surface fluxes should become feasible. This in turn will provide the basis for the quantitative understanding of the regional- and local-scale heterogeneity of the methyl bromide budget.

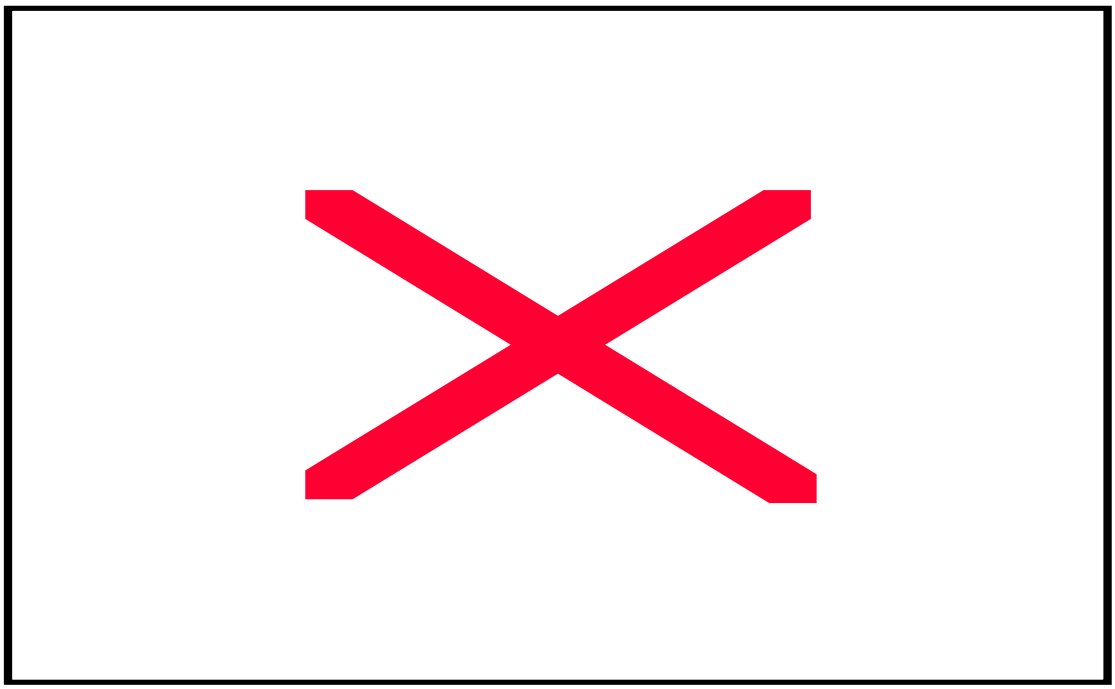

Figure 6.1. Location of NOAA-CMDL (***N***) and AGAGE (***A***) *in situ* halocarbon measurement stations. Sites where both networks have measurement stations are indicated with a (***B***).

Acknowledgements

This thesis is primarily a synthetic endeavor, and as such would not be possible without the many talented individuals who have contributed to its constituent parts. First, I must thank Ben Miller of Scripps Institution of Oceanography, and Simon O'Doherty and Peter Simmonds of the University of Bristol, for allowing me the use of their data. Natalie Mahowald (now at University of California, Santa Barbara) and Brian Eaton of NCAR provided invaluable instruction and support in the use of the MATCH model. The photolysis coefficients provided by Amram Golombek are greatly appreciated, as are the hydroxyl radical fields of Mark Lawrence of the Max Plank Instuit, Mainz. I must also thank Chien Wang of MIT, Seth Olsen and Michael Prather of the University of California, Irvine, Charles Jackman of the Goddard Space Flight Center, and Debra Weisenstein and Courtney Scott of Atmospheric and Environmental Research, Inc. for providing additional OH data, as well as Steve Montzka and Jim Elkins for their discussion of unreleased CMDL methyl bromide measurements. Finally, I thank my advisor, Ron Prinn, who always found time in his busy schedule to discuss my research, and my fiancé Alice Liu, for her unfailing support.

This work was supported by NASA (Grants NAGS-3974 and NAGI-2152 to MIT) and the National Science Foundation (Grant ATM-9610145 to MIT).

REFERENCES

Anbar, A.D., Y.L. Yung, and F.P. Chavez, Methyl bromide: Ocean sources, ocean sinks, and climate sensitivity, *Global Biogeochem. Cycles*, *10*, 175-190, 1996.

Baker, J.M., C.E. Reeves, S.A. Penkett, L.M. Cardenas, and P.D. Nightingale, An estimate of global emissions of methyl bromide from automobile exhausts, *Geophys. Res. Lett.*, *25*, 2405-2408, 1998.

Baker, J.M, C.E. Reeves, P.D. Nightingale, S.A. Penkett, S.W. Gibb, and A.D. Hatton, Biological production of methyl bromide in the coastal waters of the North Sea and the open ocean of the northeast Atlantic, *Marine Chemistry*, *64*, 267-285, 1999.

Baumann, H. and K.G.F. Heumann, Analysis of organobromine compounds and HBr in motor car exhaust with a GC/microwave plasma system, *Fres. Z. Anal. Chem.*, *327*, 186-192, 1987.

Blake, D.R., N.J. Blake, T.W. Smith, Jr., O.W. Wingenter, and F.S. Rowland, Nonmethane hydrocarbon and halocarbon distributions during the Atlantic Stratocumulus Transition Experiment/Marine Aerosol and Gas Exchange, June 1992, *J. Geophys. Res.*, *101*, 4501-4514, 1996.

Butler, J.H., The potential role of the ocean in regulating atmospheric CH_3Br, *Geophys. Res. Lett.*, *21*, 185-188, 1994.

Butler, J.H., and J.M. Rodriguez, Methyl bromide in the atmosphere, in *The Methyl Bromide Issue*, edited by C.H Bell, N. Price, and B. Chakrabarti, pp. 27-90, John Wiley & Sons, Chichester, UK, 1996.

Chen, T.-Y., D.R. Blake, J.P. Lopez, and F.S. Rowland, Estimation of global methyl bromide emissions: Extrapolation from a case study in Santiago, Chile, *Geophys. Res. Lett.*, *26*, 283-286, 1999.

Cicerone, R.J., L.E. Heidt, and W.H. Pollock, Measurements of atmospheric methyl bromide and bromoform, *J. Geophys. Res.*, *93*, 3745-3749, 1988.

Crutzen, P.J., and M.O. Andreae, Biomass burning in the tropics: Impact on atmospheric chemistry and biogeochemical cycles, *Science*, *250*, 1669-1678, 1990.

Da Silva, A., A. C. Young, and S. Levitus, *Atlas of Surface Marine Data 1994*, NOAA Atlas NESDIS 6, U.S. Department of Commerce, Washington, D.C., 1994.

DeBruyn, W.J., and E.S. Saltzman, Diffusivity of methyl bromide in water, *Marine. Chem.*, *57*, 55-59, 1997a.

DeBruyn, W.J., and E.S. Saltzman, The solubility of methyl bromide in pure water, 35 parts per thousand sodium chloride, and seawater, *Marine. Chem.*, *56*, 51-57, 1997b.

DeMore, W.B., S.P. Sander, D.M. Golden, R.F. Hampson, M.J. Kurylo, C.J. Howard, A.R. Ravishankara, C.E. Kolb, and M.J. Molina, *Chemical Kinetics and Photochemical Data for Use in Stratospheric Modeling*, *Evaluation No. 12*, JPL Publications 97-4, Jet Propulsion Laboratory, 1997.

Derwent, R. G., P.G. Simmonds, S. O'Doherty, P. Ciais, and D.B. Ryall, European source strengths and Northern Hemisphere baseline concentrations of radiatively active trace gases at Mace Head, Ireland, *Atmos. Environ.*, *32*, 3703-3715, 1998.

Elliot, S., and F.S. Rowland, Nucleophilic substitution rates and solubilities for methyl halides in seawater, *Geophys. Res. Lett.*, *20*, 1043-1046, 1993.

Gan, J., S.R. Yates, H.D. Ohr, and J.J. Sims, Production of methyl bromide by terrestrial higher plants, *Geophys. Res. Lett.*, *25*, 3595-3598, 1998.

Golombek, A., and R.G. Prinn, Global three-dimensional model of the circulation and chemistry of $CFCl_3$m CF_2Cl_2, CH_3CCl_3, CCl_4, and N_2O, *J. Geophys. Res.*, *91*, 3985-4001, 1986.

Golombek, A., and R.G. Prinn, A global three-dimensional model of the stratospheric sulfuric acid layer, *J. Atmos. Chem.*, *16*, 179-199, 1993.

Granier, C., W.M. Hao, G. Brasseur, and J.-F. Muller, Land use practices and biomass burning: Impact on the chemical composition of the atmosphere, in *Biomass Burning and Global Change*, edited by J.S. Levine, pp. 140-148, MIT Press, Cambridge, MA, 1996.

Grozko, W., and R.M. Moore, Ocean-atmosphere exchange of methyl bromide: NW Atlantic and Pacific Ocean studies, *J. Geophys. Res.*, *103*, 16,737-16,741, 1998.

Hack, J.J., Parameterization of most convection in the National Center for Atmospheric Research community climate model (CCM2), *J. Geophys. Res.*, *99*, 5551-5568, 1994.

Hao, W.M., and M.-H. Liu, Spatial and temporal distribution of tropical biomass burning, *Global Biogeochem. Cycles*, *8*, 495-503, 1994.

Hartley, D., and R. Prinn, Feasibility of determining surface emissions of trace gases using an inverse method in a three-dimensional chemical transport model, *J. Geophys. Res.*, *98*, 5183-5197, 1993.

Holtslag, A.A.M., and B.A. Boville, Local versus nonlocal boundary-layer diffusion in a global climate model, *J. Climate*, *6*, 1825-1842.

Jeffers, P.M., and N.L. Wolfe, Green plants: A terrestrial sink for atmospheric CH_3Br, *Geophys. Res. Lett.*, *25*, 43-46, 1998.

Khalil, M.A.K., R.A. Rasmussen, and R. Gunawardena, Atmospheric methyl bromide: Trends and global mass balance, *J. Geophys. Res*., *98*, 2887-2896, 1993.

King, D.B., and E.S. Saltzman, Removal of methyl bromide in coastal seawater: Chemical and biological degradation rates, *J. Geophys. Res*., *102*, 18,715-18,721, 1997.

Klein, L. Methyl bromide as a soil fumigant, in *The Methyl Bromide Issue*, edited by C.H Bell, N. Price, and B. Chakrabarti, pp. 191-235, John Wiley & Sons, Chichester, UK, 1996.

Kourtidis, K., R. Borchers, and P. Fabian, Vertical distribution of methyl bromide in the stratosphere, *Geophys. Res. Lett.*, *25*, 505-508, 1998.

Lal, S., R. Borchers, P. Fabian, P.K. Patra, and B.H. Subbaraya, Vertical distribution of methyl bromide over Hyderabad, India, *Tellus*, *46B*, 373-377, 1994.

Lawrence, M.G., Photochemistry in the tropical Pacific troposphere: Studies with a global 3D chemistry meteorology model, Ph.D. thesis, Georgia Institute of Technology, Atlanta, GA, 1996.

Lawrence, M.G., P.J. Crutzen, P.J. Rasch, B.E. Eaton, and N.M. Mahowald, A model for studies of tropospheric photochemistry: 1. Description and global simulation characteristics, submitted to *J. Geophys. Res.*, 1998a.

Lawrence, M.G., P.J. Crutzen, P.J. Rasch, and B.E. Eaton, A model for studies of tropospheric photochemistry: 2. Comparison to observations and effects of horizontal resolution, submitted to *J. Geophys. Res.*, 1998b.

Lee-Taylor, J.M., S.C. Doney, G.P. Brasseur, and J.-F. Muller, A global three-dimensional ocean-atmosphere methyl bromide distributions, *J. Geophys. Res*., *103*, 16,039-16,057, 1998.

Levitus, S., and T. Boyer, *World Ocean Atlas 1994*, NOAA Atlas NESDIS 4, U.S. Department of Commerce, Washington, D.C., 1994.

Li, Y. F., Global population distribution database: A report to the United Nations Environment Programme, UNEP Sub-Project FP/1205-95-12, 1996.

Liss, P.S., and L. Merlivat, Air-sea exchange rates: Introduction and synthesis, in *The Role of Air-Sea Exchange in Geochemical Cycling*, edited by P. Buat-Menard, pp. 113-129, D. Reidel, Norwell, Mass., 1986.

Lobert, J.M., J.H. Butler, S.A. Montzka, L.S. Geller, R.C. Myers, and J.W. Elkins, A net sink for atmospheric CH_3Br in the East Pacific Ocean, *Science*, *267*, 1002-1005, 1995.

Lobert, J.M., L.S. Geller, A.D. Clarke, J.H. Butler, S.A. Yvon, S.A. Montzka, R.C. Myers, and J.W. Elkins, BLAST94: Bromine latitudinal air/sea transect 1994 – Report on oceanic measurements of methyl bromide and other compounds, NOAA Technical Memorandum ERL CMDL-10, Boulder, CO, 1996.

Lobert, J.M., S.A. Yvon-Lewis, J.H. Butler, S.A. Montzka, and R.C. Myers, Undersaturation of CH_3Br in the Southern Ocean, *Geophys. Res. Lett*, *24*, 171-172, 1997.

Lovelock, J.E., Natural halocarbons in the air and in the sea, *Nature*, *256*, 193-194, 1975.

Mahowald, N.M, Development of a 3-dimensional chemical transport model based on observed winds and use in inverse modeling of the sources of CCl_3F, Ph.D. Thesis, MIT, 1996.

Mahowald, N.M., R.G. Prinn, and P.J. Rasch, Deducing CCl_3F emissions using an inverse method and chemical transport models with assimilated winds, *J. Geophys. Res.*, *102*, 28,153-28,168, 1997a.

Mahowald, N.M., P.J. Rasch, B.E. Eaton, S. Whittlestone, and R.G. Prinn, Transport of ^{222}radon to the remote troposphere using the Model of Atmospheric Transport and Chemistry and assimilated winds from the ECMWF and National Center for Environmental Prediction/NCAR, *J. Geophys. Res.*, *102*, 28,139-28,151, 1997b.

Manley, S.L., and M.N. Dastoor, Methyl halide (CH_3X) production from the giant kelp, *Macrocytis*, and estimates of global CH_3X production by kelp, *Limnol. Oceanogr.*, *32*, 709-715, 1987.

Manö, S., and M.O. Andreae, Emission of methyl bromide from biomass burning, *Science*, *263*, 1255-1257, 1994.

Matthews, E., Global vegetation and land use: new high-resolution data bases for climate studies, *J. Clim. Appl. Meteor.*, *22*, 474-487, 1983.

McKenzie, L.M., D.E. Ward, and W.M. Hao, Chlorine and bromine in the biomass of tropical and temperate ecosystems, in *Biomass Burning and Global Change*, edited by J.S. Levine, pp. 241-248, MIT Press, Cambridge, MA, 1996.

Miller, B.R., Abundances and trends of atmospheric chlorodifluoromethane and bromomethane, Ph.D. thesis, Univ. of California, San Diego, 1998.

Miller, B.R., and R.F. Weiss, Methyl bromide distributions in the surface ocean and atmosphere of the eastern Pacific off southern California, paper presented at the 1995 Methyl Bromide State of the Science Workshop, Methyl Bromide Global Coalition, Monterey, CA, June 5-7, 1995.

Moore, R.M., and M. Webb, The relationship between methyl bromide and chlorophyll α in high latitude ocean waters, *Geophys. Res. Lett.*, *23*, 2951-2954, 1996.

Olson, J.S., J.A. Watts, and L.J. Allison, Major World Ecosystem Complexes Ranked by Carbon in Live Vegetation, NDP017, Carbon Dioxide Information Center, Oak Ridge National Laboratory, Oak Ridge, Tennessee, 1985.

Oremland, R.S., L.G. Miller, P.M. Blunden, S.W. Culbertson, M.D. Coulatkis, and L.L. Janhke, Degradation of methyl bromide in anaerobic sediments, *Environ. Sci. Technol.*, *28*, 514-520, 1994.

Pilinis, C., D.B. King, and E.S. Saltzman, The oceans: A source or a sink of methyl bromide?, *Geophys. Res. Lett.*, *23*, 817-820, 1996.

Prinn, R.G., R.F. Weiss, B.R. Miller, J. Huang, F.N. Alyea, D.M. Cunnold, P.J. Fraser, D.E. Hartley, and P.G. Simmonds, Atmospheric trends and lifetime of CH_3CCl_3 and global OH concentrations, *Science*, *269*, 187-192, 1995.

Rasch, P.J., and M. Lawrence, Recent developments in transport methods at NCAR, *MPI Workshop on Conservative Transport Schemes, 2-3 June 1997*, Report No. 265, edited by Bennert Machenhauer, Max Planck Institute for Meteorology, Hamburg, Germany, 1998.

Reible, D.D., Loss of methyl bromide to the atmosphere during soil fumigation, *J. Hazardous Mater.*, *37*, 431-444, 1994.

Scarratt, M.G., and R.M. Moore, Production of methyl chloride and methyl bromide in laboratory cultures of marine phytoplankton, *Marine Chem.*, *54*, 263-272, 1996.

Seiler, W., and P.J. Crutzen, Estimates of gross and net fluxes of carbon between the biosphere and atmosphere from biomass burning, *Climate Change*, *2*, 207-247, 1980.

Serca, D., A. Guenther, L. Klinger, D. Helmig, D. Hereid, and P. Zimmerman, Methyl bromide deposition to soils, *Atmos. Environ., 32*, 1581-1586, 1998.

Shorter, J.H., C.E. Kolb, P.M. Crill, R.A. Kerwin, R.W. Talbot, M.E. Hines, and R.C. Harriss, Rapid degradation of atmospheric methyl bromide in soils, *Nature, 377*, 717-719, 1995.

Simmonds, P.G., S. O'Doherty, J. Huang, R. Prinn, R.G. Derwent, D. Ryall, G. Nickless, G., and D. Cunnold, Calculated trends and the atmospheric abundance of 1,1,1,2-tetrafluoroethane, 1,1-dichloro-1-fluoroethane, and 1-chloro-1,1-difluoroethane using automated in-situ gas chromatography-mass spectrometry measurements recorded at Mace Head, Ireland, from October 1994 to March 1997, *J. Geophys. Res., 103*, 16029-16037, 1998.

Singh, H.B., L.J. Salas, and R.E. Stiles, Methyl halides over the Eastern Pacific (40˚N-32˚S), *J. Geophys. Res., 88*, 3684-3690, 1983.

Wang, C., R.G. Prinn, and A. Sokolov, A global interactive chemistry and climate model: Formulation and testing, *J. Geophys. Res., 103*, 3399-3417, 1998.

Wanninkhof, R., Relationship between wind speed and gas exchange over the ocean, *J. Geophys. Res., 97*, 7373-7382, 1992.

Wingenter, O.W., .C.J.-L. Wang, D.R. Blake, and F.S. Rowland, Seasonal variations of tropospheric methyl bromide concentrations: Constraints on anthropogenic input, *Geophys. Res. Lett., 25*, 2797-2800, 1998.

WMO, Scientific Assessment of Ozone Depletion: 1994, World Meteorological Organization, Global Ozone Research and Monitoring Project Report No. 37, Geneva, 1995.

WMO, Scientific Assessment of Ozone Depletion: 1998, World Meteorological Organization, Global Ozone Research and Monitoring Project Report No. [ ], Geneva, 1999.

Yagi, K., J. Williams, N.Y. Wang, and R.J. Cicerone, Atmospheric methyl bromide (CH_3Br) from agricultural soil fumigation, *Science, 267*, 1979-1981, 1995.

Yvon, S.A., and J.H. Butler, An improved estimate of the oceanic lifetime of atmospheric CH_3Br, *Geophys. Res. Lett., 23*, 53-56, 1996.

Zhang, G.J., and N.A. McFarlane, Sensitivity of climate simulations to the parameterization of cumulus convection in the Canadian Climate Centre general circulation model, *Atmos.-Ocean, 33*, 407-446, 1995.